



Optimizing Induction Heating for Manganese Steel for Induction Assisted Machining

By

Ravshan Yakupov

CODEN: LUTMDN/ (TMMV-5352)/1-82/2023
Department of Production and Materials Engineering
Faculty of Engineering, LTH, Lund University
SE-221 00 Lund, Sweden

Abstract

The main factors for usage of Induction assisted machining of Manganese steel were identified in this project. The testing environment to evaluate performance of the high frequency coils for turning and milling was created. The characteristics of the material that we are working with were measured. Such variables as the cutting speed, feed rate, area to be heated and the time of the heating on the desired area were identified as the most critical variables for the design of the coil. To reach fast heating speed and not to go deep into the material, high frequencies are preferred, high frequencies will allow concentrating the fluxes on the desired depth, which will not go further into the workpiece and will not deteriorate the properties of the material. The strain hardening phenomena can be avoided by use of the induction assisted machining, as it will soften already strain-hardened material. Concept of the high frequency coil was proposed and key factors for the successful preheating of M1 manganese steel were identified. Further basis of reinforced M1 manganese steel induction assisted machining was developed.

Keywords: induction assistive machining, induction assisted machining, manganese steel, preheating, induction coil, reinforced material

Acknowledgments

I would want to extend my sincere gratitude to everyone who helped me complete my degree project and who offered encouragement and direction.

First, I would want to express my sincere gratitude to my supervisor, Volodymyr Bushlya, for his constant advice, knowledge, and support. His insightful opinions, helpful criticism, and consistent availability have been crucial in determining the direction of this project.

I would especially like to thank Ville Akujärvi and Tord Cedell for their contributions to the lab and their time. I also want to express my gratitude to Mikael Hörndahl, Andrii Hrechuk, Ryszard Wiezbicki and Klas Holger Jönsson for their suggestions and significant assistance in the fabrication of the necessary elements. In addition, I would like to express my thanks to Kenneth Frogner, for his help and expertise related to the power supply configurations.

Additionally, I would like to express my profound gratitude to everyone at the Department of Production and Materials Engineering for their commitment to fostering an academic environment that is stimulating and to education. Their expertise, enthusiasm, and eagerness to impart it have been priceless assets that have improved my learning process.

I am really appreciative of my parents and the people in my life for their love, support, and confidence in me.

In closing, I would want to express my sincere gratitude to everyone who has helped in any way, whether it was obvious or not. Without their assistance, this project would not have been possible, and I consider myself incredibly lucky to have had the opportunity to collaborate with such amazing people.

Thank you all.

Ravshan Yakupov

Contents

Abstract	2
Acknowledgments	3
Table of figures	6
List of tables	9
Abbreviations	9
1. Introduction	11
1.1. Background	11
1.2. Problem description.....	11
1.3. Project goal and objectives.....	12
1.4. Limitations	13
1.5. Challenges	13
2. Theoretical Background and Literature Review.....	14
2.1. Metal cutting theory	14
2.2. Basic concepts	17
2.3. Material related information.....	25
3. Research instrumentation	30
3.1. Material characterization equipment	30
3.2. Milling imitation machine	31
3.3. Thermal measurements equipment.....	33
4. Conducted experiments	36
4.1. Material measurements.....	36
4.2. Low frequency IAM imitation	38
4.3. High frequency milling coil	42
4.4. High frequency turning coil	49
4.5. Analysis of conducted experiments.....	55
5. Iterations in the design and use of the coils.....	58

5.1. Milling coil issues and modifications.....	58
5.2. Experimental validation of high frequency induction coil for turning	64
6. Results and discussions	72
7. Conclusion.....	76
8. Outlook.....	78
References	81

Table of figures

Figure 1 Definition of the major chip area parameters in the axial direction for turning (St åhl, 2012).....	14
Figure 2 Simplified scheme of milling process (Stjernstoff, 2004) ..	16
Figure 3 Different kinds of reinforcement types: a) continuous long fibers, b) discontinuous short fibers or whiskers and c) particles in the matrix (Dieringa, 2012).....	17
Figure 4 SEM images of Manganese based MMC reinforced with Tungsten carbide (HEMA KALIDASU, 2021)	18
Figure 5 Semicircular induction coil (Baili M, 2011).....	20
Figure 6 Cutting forces for different depth of cut and machining methods (Eun-Jung Kim, 2020)	21
Figure 7 Coil design used by Kim et.al., Baek et.al. (Jong-Tae Baek, 2018).....	22
Figure 8 Cutting forces for Inconel 718, different machining methods and different depth of cut (Jong-Tae Baek, 2018)	22
Figure 9 Maximum size of tool wear and surface roughness of Inconel 718 (Jong-Tae Baek, 2018)	23
Figure 10 Comparison of cutting forces and tool life for the machining under room temperatures and the preheating with induction (M.I. Hossain, 2008)	23
Figure 11 Induction coil set up used by Ginta et.al. and Hossian et.al. (M.I. Hossain, 2008)	24
Figure 12 SEM views of flank wear: (a) at room temperature after 1990 mm length of cut, (b) with preheating at 650 °C after 4200 mm length of cut (Turnad L. Ginta, 2009)	24
Figure 13 SEM of crater wear (Turnad L. Ginta, 2009)	25
Figure 14 Metallographic photo of medium manganese austenitic steel (Shirong Ge, 2017).....	26
Figure 15 Influence of the tool on hardening of the workpiece surface (Kopac, 2001).....	27
Figure 16 Hardness of Mn-steel at different temperatures (J. Kopac, 1983).....	28
Figure 17 Ultra-precision scales for density measurements.....	30
Figure 18 Netzsch LFA 467	30

Figure 19 Schematic of the LFA 467 HT HyperFlash; the light beam heats the lower sample surface and an IR detector measures the temperature increase on the upper sample surface (Netzsch)	31
Figure 20 Pencil machine for the testing of the coils	32
Figure 21 a) DC motor for movement in y direction b) control box.	32
Figure 22 a) PLC b) current control device.....	33
Figure 23 Travelling range of the table in y-directions.....	33
Figure 24 FLIR ThermoCAM T360.....	33
Figure 25 Workpiece in form of rectangular slab	34
Figure 26 Master Spray Paint 600 °Svart.....	34
Figure 27 Prepared workpiece with glued thermocouples	35
Figure 28 Measured thermal diffusivity, thermal conductivity and specific heat capacity of M1 steel and reinforced material	37
Figure 29 Chemical composition of M1 steel	37
Figure 30 Fully assembled testing equipment (Low frequency heating unit)	39
Figure 31 Measured temperatures by thermocouples. ch0- ch4 corresponds to the thermocouples placed on the surface, while ch5- ch8 are the ones on the bottom.....	40
Figure 32 Heat pattern of low frequency heating unit, under the speed of 600mm/min	41
Figure 33 Draft version of the HF milling coil design. a) Front view, b) Up view, c) Side view, d) section view, e) power source connectors , and water- in -out adapters	42
Figure 34 Separate parts for the milling coil.....	43
Figure 35 High frequency coil for milling	43
Figure 36 Induction frequency inverter	44
Figure 37 Set up for the milling coil testing.....	44
Figure 38 Heat pattern, under the current of 15A	45
Figure 39 Heat pattern, under the current of 18A	46
Figure 40 Heat pattern, under the current of 20A	46
Figure 41 Heat pattern, under the current of 25A	47
Figure 42 Heat pattern, under the current of 35A	47
Figure 43 Heat pattern, under the current of 38A	48
Figure 44 Heat pattern, under the current of 40A	49
Figure 45 High frequency coil for turning	50
Figure 46 Point of the highest temperatures in the heating unit.....	51
Figure 47 $V_c=1000\text{mm/min}$, Current 18A.....	52

Figure 48 Cooling added to the lid.....	52
Figure 49 Experiments with added cooling system to the lid	54
Figure 50 Melted path	55
Figure 51 Control inputs used for induction heating processes (Faulkner, 2007).....	56
Figure 52 Milling coil testing set up	59
Figure 53 Paralleled capacitors and transformers and as the series to coil.....	60
Figure 54 Design of the cooler for the ferrite.....	61
Figure 55 3D printed ferrite cooler	61
Figure 56 Current of 25A, power output 10kW, maximum temperatures of the workpiece 260-270°C	62
Figure 57 Current of 27A, power output 12kW, maximum temperatures of the workpiece 290-300°C	62
Figure 58 Current of 29A, power output 14kW, maximum temperatures of the workpiece 320-330°C	63
Figure 59 Current of 29A, power output 14kW, feed rate 0.6 m/min, maximum temperatures of the workpiece 380°C-400°C.....	63
Figure 60 SMT turning lathe.....	64
Figure 61 Workpiece mounted into lathe.....	64
Figure 62 Conceptual design for the HF coil holder. a) Attachment to the SMT machine. b) Rack for coil fixturing attachment and axial distance control. c) Rack for the perpendicular take out of the coil, to avoid collision with the tool. d) Assembled version.	65
Figure 63 Holder for the HF turning induction coil. a) Is attached to the SMT tool holder, for the movement along with the tool. b) Hole is made to control the distance of the coil to the workpiece. c) Coil fixturing, also possible to control the distance to the workpiece. d) Gives possibility to control distance of the coil in axial direction. ...	66
Figure 64 IR camera image, temperature pattern under the current of 30A	67
Figure 65 IR camera image, temperature pattern under the current of 32A	67
Figure 66 IR camera image, temperature pattern under the current of 40A	68
Figure 67 IR camera image, temperature pattern under the current of 40A, decreased rotational speed of 160rpm	68
Figure 68 Damage on the tip of ferrite	69

Figure 69 Failure of the coil.....	70
Figure 70 Core damage	71
Figure 71 Dependencies in induction heating, 1-3- low frequency heating unit, 4-5 – high frequency milling coil, 6-7 high frequency turning coil in SMT, 8-HF coil for turning in pencil machine. Blue- feed rate, velocity (m/min), red- peak temperatures reached(C°), green – heated area,(mm ²).....	72
Figure 72 Simulation of heating depth dependence on time, in the current set up and the workpiece.....	74
Figure 73 Suggested design for the coil. a) front view b) side view c) bottom view d) 3D model.....	78
Figure 74 a) section view, b) front view	79
Figure 75 View from above before bending	79

List of tables

Table 1 Tabulated data as function of temperature for the tested materials	38
Table 2 Tabulated data for comparison of different conditions	72

Abbreviations

WP – workpiece

A – chip area

a_p – depth of cut

f – feed

b_1 – underformed chip width

h_1 –theoretical chip thickness

v_c – cutting speed

V_f – feed rate

a_e – width of cut

MRR – Material Removal Rate

HAM – Heat assisted Machining

IAM – Induction assistive machining/ Induction assisted machining

MMC – Metal Matrix Composites

LAM – Laser assisted machining/ Laser assistive machining

CM – conventional machining

FEA – Finite element analysis

IR – infrared

HF – high frequency

1. Introduction

In the upcoming chapter, degree project will be presented in a structured manner, consisting of various sub-chapters that cover brief overview and identification of the problem, the project objectives, and limitations that are currently connected with a topic.

1.1. Background

Nowadays increase in metal matrix composites can be observed in the industry, due to superb performance of such materials, and characteristics that can be tailored for specific tasks. However, it is clearly seen the lack of machining methods and difficulties connected with machining of them, which in result effects the part costs and quality of it.

The implementation of assistive technologies can give us gain in terms of tool performance, final part cost, even the possibility for the machining of some material and in overall better optimization of manufacturing processes. Method of Induction assisted machining will be analyzed, as it is playing a key role in this project, which can be implemented in different cutting operations and have a high scope of use and predicts to have positive performance improvement.

The implementation of induction to preheat the material will have an exploratory character, and by the end of the work, kinematic model with reference to high content manganese steel will be developed, and proven experimentally.

1.2. Problem description

1.2.1 Material related difficulties

Original purpose of the material that we are currently working with is that it will be used to produce conical stone crusher and it is machined by conventional machining method, which results in high production cost and requires long time to produce final product. Inserts that are used now are not capable to withstand the load during manufacturing process, resulting in short tool life, due to fast

deterioration because of high cutting forces affecting it, and as result, they should be changed very often.

Another key problem is an introduction of the new material, which is reinforced version of previously used high manganese steel version. Reinforced material should give better performance of the final product, and currently it is impossible to machine it with standard methods.

Main issue with current material, which is high manganese austenitic steel, is that it has tendency to the material hardening during cutting processes, due to high material deformation in the cutting zone. At a low cutting depth plastically deformed or degenerated layer can appear. In addition, diffusion wear can be observed during machining of Mn-steels (Kopac, 2001).

1.2.2 Induction assistive machining

Up to date, there is no universal solution for the induction coil design that can be used at any environment and suitable for all machining processes. In addition, when we are working with Mn-steels, induction should be on optimal level of depth, temperature, time, as manganese steels have a tendency to hardening, and change of the characteristics on certain range of temperatures. Therefore, the coil should induce the material with controlled depth, temperatures, and short period of time that will give us possibility to machine reinforced particles. Consequently, tailored solution for different type of materials and processes is usually made.

1.3. Project goal and objectives

Project is aimed on the development and optimization of the heat distribution by the use of induction assistive machining with reference to M1 manganese steel.

As there is no existing basis for the project, following objectives can be outlined and developed on the upcoming basis.

- Create a testing environment for such processes as turning and milling, with respect to induction assisted machining.

- Constructing and experimenting with induction heating solutions tailored to specific process movements, and their analysis.
- Check the possibility of universal design for the induction coil, which can be used in different environment.

1.4. Limitations

Current project will consider behavior of the heating process with the help of induction. Imitation of Induction assistive milling and turning will be concluded, and the testing facility for it would be produced and organized.

Knowledge basis and engineering solution will be provided, by approaching experiments under different environment and set ups, and further analysis of them would be done.

1.5. Challenges

Due to the complicated nature of the current tasks, there is a lack of literature and previous research on induction-assisted machining of manganese steels. The current materials being used are new materials designed by SANDVIK SRP. Usually, building an induction heating coil in a small-scale laboratory environment is challenging, but it needs to be done to prove the efficiency of the method. The lack of material supply for the ferrites and the complicated form of the coil are also obstacles for this thesis.

The inverters that are typically used are not supposed to be used in this industry. They are preferred for use with composites heating, which requires much lower temperatures. Therefore, a completely new setup needs to be built. Since ranges of high frequencies need to be used, significant heat would be generated by the coil components. Considering laboratory conditions, it would be difficult to build different options and test them within the time period of the research.

2. Theoretical Background and Literature Review

Chapter will represent literature research that was done to identify key factors for the topic of this thesis and analysis of previous experience in induction assisted machining of different materials. Although some literature about steel with high manganese content would be analysed to understand the behaviour of material, so the assumption of the material can be drawn. In addition, basic concept of the processes would be described.

2.1. Metal cutting theory

Machining can be described as a shearing process where chips are formed. There are number of different machining processes, they can be subdivided into two groups. One of them is continuous (turning, drilling) and another is non-continuous (milling, sawing, grinding).

Turning

Turning is a metal cutting process in which cutting tool, typically a single point cutting tool, is used to remove material from a rotating workpiece. The cutting tool is fed into the workpiece(WP) longitudinally, and fixed on the radial distance to the WP, removing material in the form of chips to achieve desired shape and surface finish (Ståhl, 2012).

During the turning process, the WP is mounted on a lathe, which rotates the WP at a constant speed while the cutting tool moves along the length of the WP to remove the material. The cutting tool is held in a tool post, which can be adjusted to control depth and angle of the cut (Ståhl, 2012).

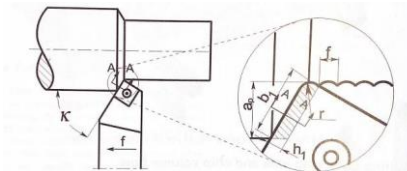


Figure 1 Definition of the major chip area parameters in the axial direction for turning (Ståhl, 2012)

For the turning process, chip area, and in some sense area of contact between tool and the WP can be calculated by Equation (1).

$$A \approx a_p \cdot f \approx b_1 \cdot h_1 \quad (1)$$

Based on the Eq.1, we can configure the speed of how fast can be the turning process executed, by adding one more variable, which is cutting speed(v_c), which means how fast would be the tool moving along the surface of the WP , Equation(2) (Stahl, 2012).

$$MRR \approx A \cdot v_c \approx a_p \cdot f \cdot v_c \approx b_1 \cdot h_1 \cdot v_c \quad (2)$$

In the end, it will give us understanding of Material Removal Rate (MRR), which is one of the key characteristic in manufacturing process. Higher MRR and longer tool life will always gain us better economic performance and will save a lot of time to produce the end product. Thereby with introducing induction assisted machining (IAM) into the turning, possibility to improve MRR appears, as assistive machining will give more freedom in terms of variation of all the cutting data to be set up.

Milling

Milling is a machining process that involves the use of a rotating cutting tool to remove the material from the WP. It is a versatile process that can be used to create a wide range of shapes, sizes and features in metal or other materials (Stahl, 2012).

In a milling machine, the WP is held stationary while the cutting tool rotates and removes the material from the surface of the WP, also an option where the WP is driven by the table in which it is mounted to and the spindle is rotating and material is removed when the table is fed to the tool.

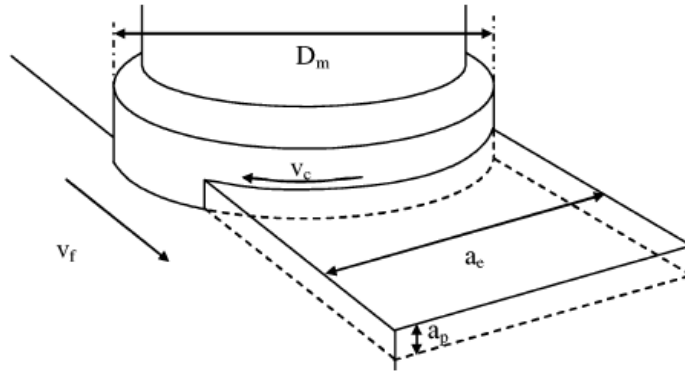


Figure 2 Simplified scheme of milling process (Stjernstoff, 2004)

For the interest of the current project, parameters that will play significant role are a_p , a_e , V_f , which are depth of cut, engagement area and feed rate respectively. Should be noted that in milling feed rate can be counted as how fast the spindle is moving on to the fixed WP, or how fast WP is fed to the rotating spindle.

In milling depending on the number of inserts and the spindle rotation speed, we can adjust the feed rate (V_f). Material characteristics also plays significant role in determining of all the parameters, so for our interest in relation with induction heating, material will be softer so the parameters of depth of cut (a_p), and width of cut (a_e) can be increased. Which will increase the MRR, Equation (3).

$$MRR \approx a_e \cdot V_f \cdot a_p \quad (3)$$

Material removal rate

Material removal rate is a key metric in metal cutting that refers to volume of material that is removed from the WP per unit time during a cutting operation. MRR is an important factor in metal cutting operations as it directly influences efficiency, productivity, and cost-effectiveness of the process (Stahl, 2012).

MRR is influenced by several factors, including the cutting conditions, the properties of the WP material, and the type of cutting tool to be used. The cutting conditions, such as cutting speed, feed rate, and depth of cut, have direct impact on MRR. Higher cutting speeds, feed rates, and depths of cut generally result in higher MRRs. However,

it is important to balance these factors with the need to maintain tool life and achieve good surface finish. The properties of the WP material also play a role in determining MRR. Materials with higher strength and hardness generally require lower cutting speeds and feed rates to avoid excessive tool wear and damage.

MRR for the turning can be configured in two ways by varying the cutting speed and chip area. Adjusting chip area affects the chip thickness and width, and consequently the MRR, while modifying the cutting speed, which is combination of feed rate and rotational speed of the WP, influences the machining time and subsequently the MRR. Careful optimization of these parameters is crucial to achieve the desired material removal rate while maintaining appropriate cutting conditions and maximizing productivity.

2.2. Basic concepts

As the basic purpose of this study is adopting induction assisted machining (IAM) to be used with metal matrix composites (MMC), basic understanding of it should be provided. It is a class of materials known as metal matrix composites, consist of a metal matrix reinforced with the secondary phase, usually ceramics fibers or particles.

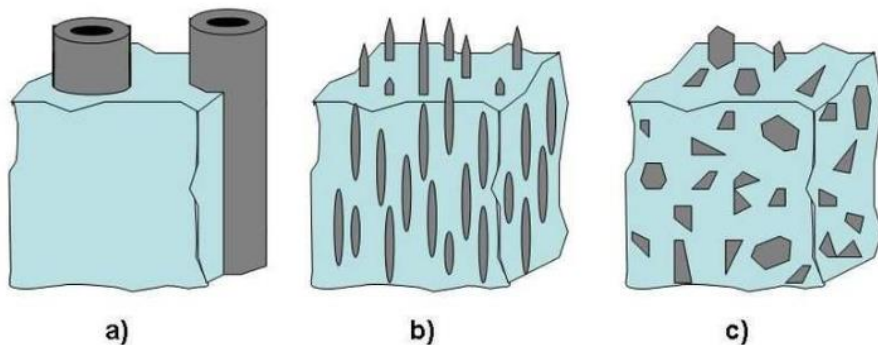


Figure 3 Different kinds of reinforcement types: a) continuous long fibers, b) discontinuous short fibers or whiskers and c) particles in the matrix (**Dieringa, 2012**)

The volume fraction, size and distribution of the reinforcing phase, as well as the makeup of the metal matrix, can all be changed to customize the properties of MMCs. In general, MMCs have stronger,

stiffer, and more wear-resistant mechanical characteristics as compared to their monolithic metal counterparts. MMCs can also have exceptional corrosion resistance, outstanding thermal and electrical conductivity, and both (Gupta, 2021).

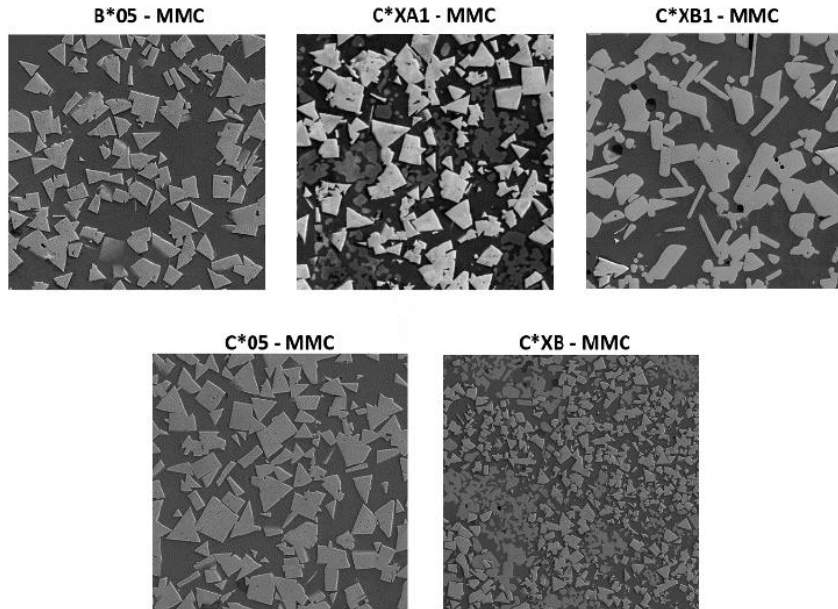


Figure 4 SEM images of Manganese based MMC reinforced with Tungsten carbide (HEMA KALIDASU, 2021)

Due to their unique properties, MMCs have found a wide range of applications in industries such as aerospace, automotive, and electronics. For example, MMCs have been used in the production of engine components, brake discs, heat sinks, and printed circuit boards (Prof A. N. Purant, 2020).

Machining of MMC can be a challenging process due to the presence of the reinforcing phase, which can cause excessive tool wear and damage to the WP. However, with proper selection of machining parameters and cutting tools, high-quality MMC components can be produced.

Some important considerations when machining MMCs include the selection of appropriate cutting tools and machining parameters, such as cutting speed, feed rate, and depth of cut.

Overall, machining MMCs can be a challenging process, but with proper selection of cutting tools and machining parameters, and in our case adding up of the heat assistance to soften the material and reinforced particles in it, high-quality components with improved mechanical properties can be produced.

Induction assisted machining is a subdivision of heat assisted machining which is a technique that involves the use of localized heating to reduce the cutting forces and improve the machinability of difficult-to-machine materials, such as MMCs. In heat assisted machining (HAM), a heat source, such as a laser or an induction heater, is used to heat the WP material to a temperature below its melting point but high enough to soften the matrix material and reduce the strength of the reinforcing phase.

HAM can improve the machinability of MMCs by reducing the cutting forces and tool wear, as well as improving surface finish and dimensional accuracy. Additionally, HAM can reduce the risk of micro-cracks or delamination of the composite during machining, which can be particularly important for producing high-quality parts.

Several factors need to be considered when using HAM for machining MMCs, including the selection of an appropriate heat source, the power and duration of the heat input, and the cooling rate after machining. The heat input needs to be carefully controlled to avoid thermal damage of the WP, and the cooling rate needs to be optimized to avoid the formation of residual stresses or distortion.

One disadvantage of HAM is the increased cost and complexity of the machining process due to the need for specialized equipment and the added time required for heating and cooling. However, for certain applications where high quality, complex MMC components are required, HAM can offer significant benefits over conventional machining techniques.

Induction heating is a non-contact heating process that uses induced electromagnetic current (eddy currents) to bond, soften or harden electrically conductive material. Induction heating have such pluses as controllability, speed of heating and heat distribution, which makes it one of the supreme methods for the assistive heating during the machining processes (Armin Bijanzad, 2022). Induction heating have a good potential for the use in industry and several researches

were done for investigation of the induction heating with the machining of superalloys.

Baili et.al. (Baili M, 2011) performed hot machining with induction of the Ti-5553, semi-circular induction coil was integrated, which partial enveloped the WP for pre-heating during turning operation.

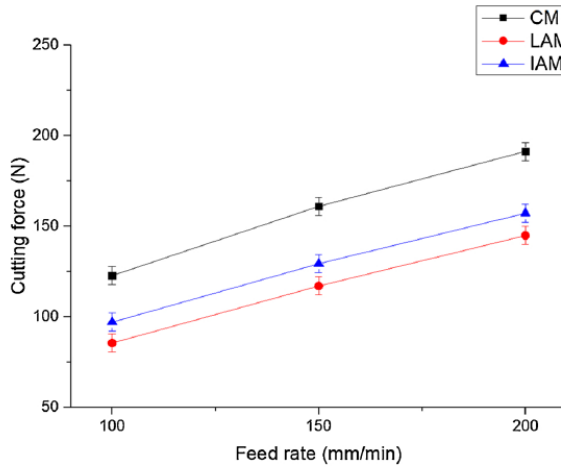


Figure 5 Semicircular induction coil (Baili M, 2011)

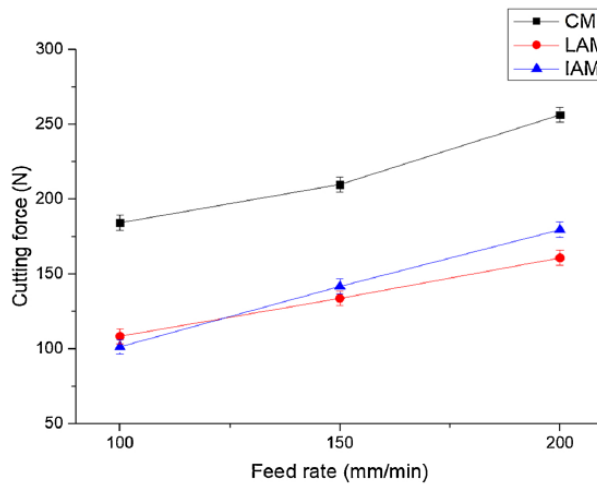
It gave an advantage of heating and cutting at the same time, partially involving WP for preheating, which gave homogeneous heat distribution on the material. For the titanium, desired temperatures were above 600°C as it start to soften at this point, and significant decrease in measured forces were observed. When temperatures were reached up to 800°C decrease in forces were about 40% in comparison with 500°C . However, as result of this research, tool life was reduced due to change in material structure that was caused by the temperature.

Kim et.al. (Eun-Jung Kim, 2020) made a research about induction assisted heating in milling process. The purpose was to investigate the power consumption during machining process and compare it with laser assisted machining (LAM). Result of this work showed that LAM is more efficient in terms of power consumption. For IAM suggestion is to use deeper depth of cut in comparison with LAM, but lower feed rate should be used, due to time that is required for heating which is enough for oxidation of the upper layer of WP that can give bad results.

Main interest in this work was decrease in cutting forces, which plays significant role in our case.



(a) Depth of cut set at 0.25 mm



(b) Depth of cut set at 0.5 mm

Figure 6 Cutting forces for different depth of cut and machining methods (**Eun-Jung Kim, 2020**)

This research showed efficiency of LAM and IAM in comparison with conventional machining (CM), and even with taking into account

that LAM would be more efficient in terms of power consumption and machinability, the efficiency would not outweigh the cost of the process, as IAM is about 10 times cheaper than LAM.



Figure 7 Coil design used by Kim et.al., Baek et.al. (**Jong-Tae Baek, 2018**)

Baek et.al. (Jong-Tae Baek, 2018), made a work to compare machining of AISI 1045 steel and Inconel 718 with IAM and LIAM and with conventional machining without preheating. Induction heating was used to soften and reduce mechanical strength of the material, FEA was performed in this research to confirm efficient depth of cut, which was done to identify efficient depth of cut for different temperatures. Research showed such results as decrease in cutting forces up to 80% in comparison with CM. Surface quality and the tool wear were also enhanced greatly in comparison with CM, which proved that IAM and Laser Induction Assisted Machining are more effective methods to improve tool life and surface quality. Figure8-9

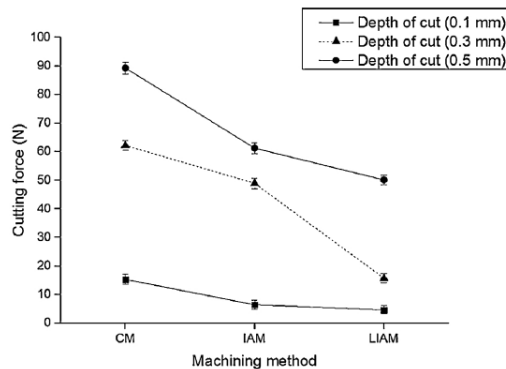


Figure 8 Cutting forces for Inconel 718, different machining methods and different depth of cut (**Jong-Tae Baek, 2018**)

	Conventional machining	Induction assisted machining	Laser-induction assisted machining
Tool wear (mm)	0.288	0.341	0.225
Surface roughness, Ra (μm)	0.711	0.437	0.281

Figure 9 Maximum size of tool wear and surface roughness of Inconel 718 (**Jong-Tae Baek, 2018**)

High frequency induction heating was proven to be efficient in terms of increasing of the tool life, lowering down the cutting forces and decreasing amplitude of the vibrations, it also helped to reduce the strain hardening of the material, experiments were done with Ti-6Al-4V and the preheating temperature was 420°C, Hosain et.al. (M.I. Hossain, 2008)

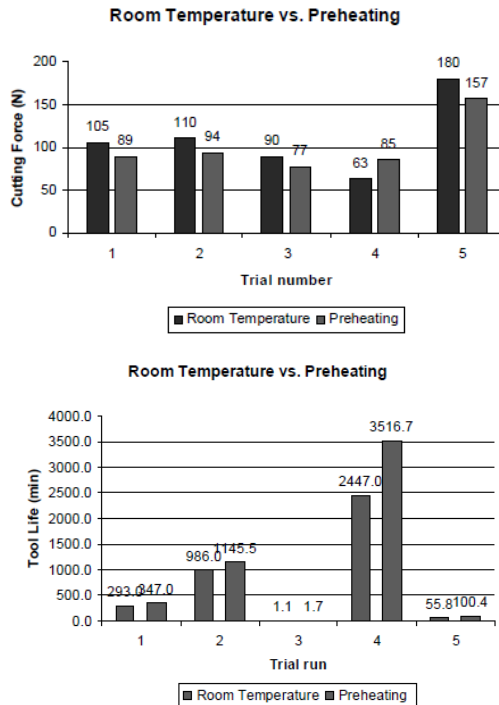


Figure 10 Comparison of cutting forces and tool life for the machining under room temperatures and the preheating with induction (**M.I. Hossain, 2008**)

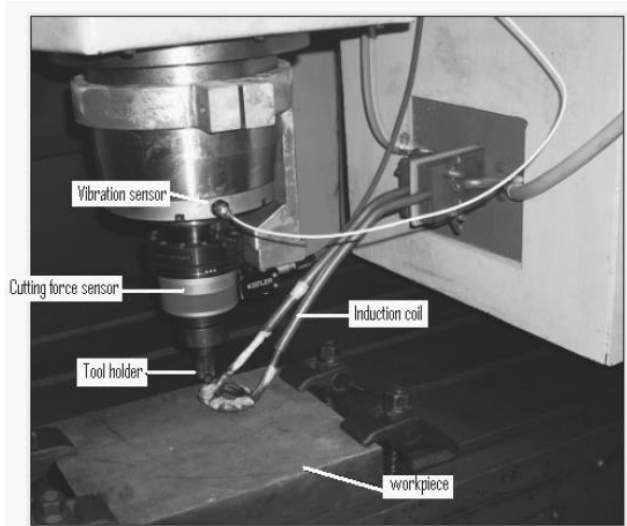


Figure 11 Induction coil set up used by Ginta et.al. and Hossian et.al. (**M.I. Hossain, 2008**)

Ginta et.al. (Turnad L. Ginta, 2009), also done very similar research with same material but different insert (PCD), and higher temperatures (650°C), increase in tool life was almost 2.7 times compared with conventional machining, all other benefits were almost same as at Hosain et.al.'s work, lowering of cutting forces and reducing of vibrations.

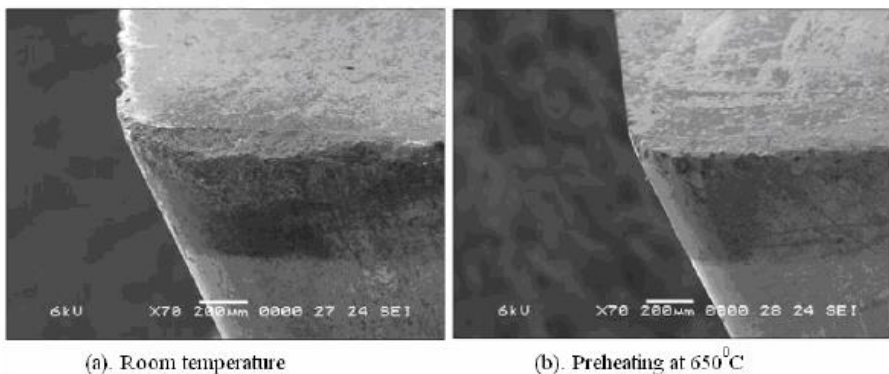


Figure 12 SEM views of flank wear: (a) at room temperature after 1990 mm length of cut, (b) with preheating at 650 °C after 4200 mm length of cut (**Turnad L. Ginta, 2009**)

It is also can clearly be seen from Figure 12 and Figure 13 that due to preheating of the material less damage was done to the tool even under longer period of machining.

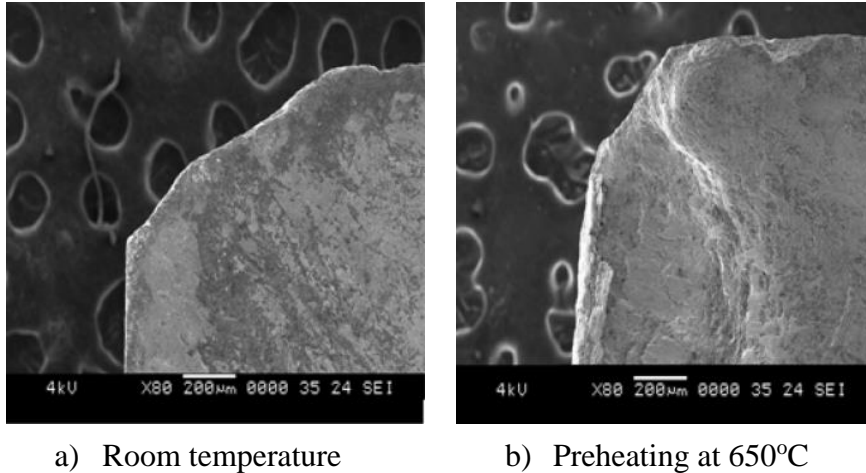


Figure 13 SEM of crater wear (Turnad L. Ginta, 2009)

In overall most of the researches shows that IAM has big potential and can be used for machining of hard to machine materials, but it requires some development in terms of mobility of the coil, and better universality of the use which will increase the scope of use and the scale for the size of the WP. In addition should be said that in most of conducted studies depth of heating was not an issue, because materials that were in the scope of the researchers' interest do not have a deterioration tendency under effect of high temperatures, which in our case is one of the main factors, so depth penetration of the heat should be controlled.

2.3. Material related information

Mangalloy has very high tensile strength and fair yield strength. Depending on the percentage of manganese and other elements. Alloys can be divided into three application groups:

Working in an abrasive environment with relatively small specific loads.

Working in an abrasive environment with significant shock loads.

Working in an abrasive environment with very significant alternating loads and specific pressures.

Such characteristics can be observed in such alloys as 125G18X2L(Russian standards “125Г18Х2Л”), 110G13L(Russian standards “110Г13Л”), Hadfield steel, steel Mn17Cr15N0.43C0.39, AISI 316L stainless steel, different austenitic alloys (Titanium Alloy TA15, Inconel 718 and etc.) (M.S.Shramko, 2006).

Acselrad et.al. (Oscar Acselrada, 2004), conducted a study on behavior of FeMnAlC steel and compared it with M2 steel and AISI 304 stainless steel. All of three materials are austenitic steels, which have a low stacking fault energy, which in the end gives the superficial layer deformation and strain hardening of the material, becoming more difficult to remove and consequently making it harder for wear. Main subject of this study was to understand if FeMnAlC steel can replace other two materials, but for our interest, it is not the main point of this paper, we are more interested in behavior of the material, which was pretty similar for all three of them. Materials were designed to operate in aggressive environments, which characterizes them as wear resistant and hard to machine materials. Short exposure under the temperature of 550-700°C will strengthen the material, by forming of k-phase orientation of the structure, which is hard to remove and very abrasion resistant which makes it hard for us to machine, so heat penetration depth should be controlled for the depth of only planned to cut part.

Ge et.al. (Shirong Ge, 2017), states that medium manganese steel has a self-strengthening effect under the medium or low-impact loads as it is connect with deformation induced martensitic transformation.



Figure 14 Metallographic photo of medium manganese austenitic steel (**Shirong Ge, 2017**)

In addition, it was proven that because metallographic phase transformation has an effect of obstructing the movement of the sliding faces dislocations. Which gives deformation-induced martensite transformation, and as result enhancement of hardness and wear resistance also can be observed in these kind of steels. It can be concluded that medium manganese steel has high wear resistance rate and preferred to be used in aggressive environment, which leads to an assumption that it is hard to machine material.

Same observation was done by Janec Kopac, and the hardened layer is usually from 0.1 to 0.5mm, which is harder than the basic WP material in 2.5-2.7 times. (Kopac, 2001)

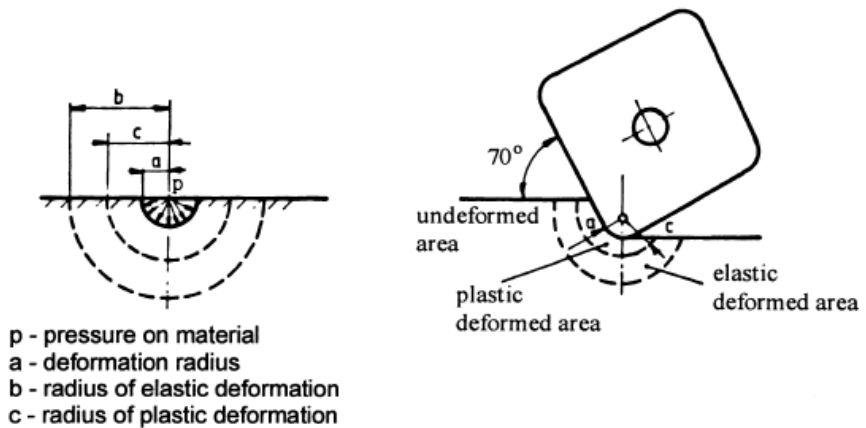


Figure 15 Influence of the tool on hardening of the workpiece surface (Kopac, 2001)

Moreover, this effect can be evaded by the preheating the WP to the temperatures of about 600°C, as it such temperatures very fast drop in hardness of the Mn-steels is observed, Figure 16.

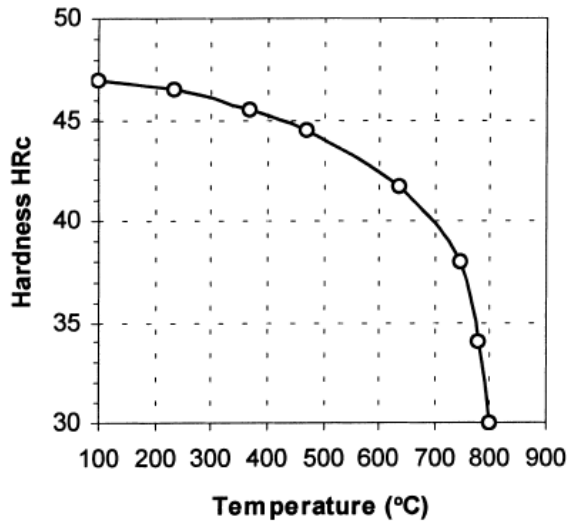


Figure 16 Hardness of Mn-steel at different temperatures (J. Kopac, 1983)

One of the key characteristics of high-medium manganese steel is its ability to work-harden, which means that it becomes harder and stronger as it is subjected to impact and stress. This work-hardening effect is due to the formation of austenite and the displacement of the manganese atoms in the lattice, which leads to the formation of dislocations and increased hardness (Kopac, 2001).

However, high-medium manganese steel can also have some drawbacks. It can be difficult to machine and weld due to its high hardness and toughness, and it is prone to cracking if not handled properly. In addition, it is typically more expensive than other types of steel due to its high manganese content.

High-medium manganese steel is a specialized type of steel that offers exceptional wear resistance and toughness in high-impact and abrasive applications, but it is important to carefully consider its properties and limitations before selecting it for a specific application (Shirong Ge, 2017).

In addition, it should be said that reinforcing particles, such as ceramics or carbides, could further increase the difficulty of machining these materials. The behavior of the cutting process of hard-to-cut materials with reinforced particles is complex and depends on a variety

of factors, including the properties of the material, the cutting conditions, and the type of cutting tool used.

When cutting hard-to-cut materials with reinforced particles, the cutting tool can experience high stresses, resulting in increased tool wear and reduced tool life. The reinforcing particles can also cause abrasion, adhesion, and chipping of the cutting tool, leading to poor surface finish and dimensional accuracy.

As a final remark based on the information presented above, the application of external heat in machining difficult-to-cut metals and alloys leads to improved machinability, which is evident through significant reductions in cutting force. Additionally, heat-assisted machining enhances tool life. Consequently, this can reduce machining lead time and lowers the overall machining cost.

The strain-hardened layer formed during conventional room temperature machining can be either completely or partially eliminated during heat-assisted machining.

In this work to overcome this challenge, IAM was chosen which is supposed to improve the cutting process and reduce the cutting forces, leading to better tool life and the possibility to machine the material itself.

3. Research instrumentation

Current chapter will introduced equipment that was manufactured and used for the experiments.

3.1. Material characterization equipment

To define the density of the WP buoyancy density measurement method was used. By use of ultra-precision scales with the accuracy of 0.0001g. Figure 17



Figure 17 Ultra-precision scales for density measurements

Thermal measurements for all of the materials were performed on the Netzsch Laser Flash Analysis LFA 467 HT HyperFlash. Figure 18



Figure 18 Netzsch LFA 467

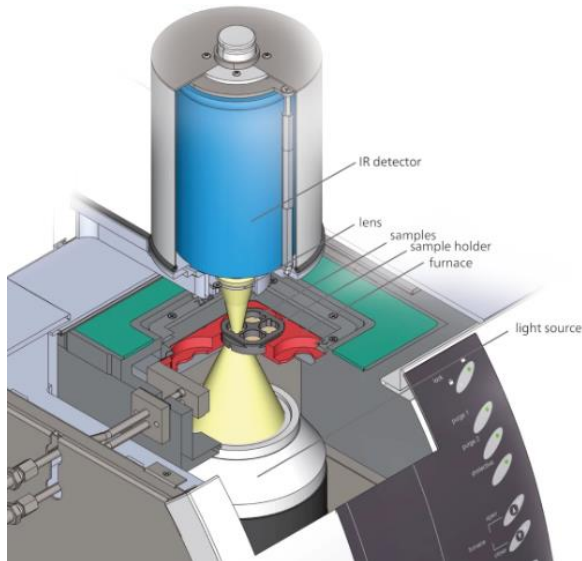


Figure 19 Schematic of the LFA 467 HT HyperFlash; the light beam heats the lower sample surface and an IR detector measures the temperature increase on the upper sample surface (**Netzsch**)

Netzsch Laser Flash Analysis LFA 467 HT HyperFlash is a lamp based LFA system, with maximum reach temperature of 1250°C and a maximum heat rate of 50K/min. Maximum data acquisition rate of 2Mhz, thermal diffusivity range from 0.01mm²/s to 2000mm²/s. thermal conductivity from less than 0.1W/(m K) to 4000W/(m K).

3.2. Milling imitation machine

For testing of the coils and spreading of the heat on the WP the pencil machine with electrical drive, Figure 20, was build, which was capable of maximum speed of 1143 mm/min. Essentially, it consists of a compact milling machine resembling a table-top setup, but with the spindle removed. Instead, a suspended arm, formerly occupied by the spindle, holds the coil. The coil can be manually lowered to a desired distance from the WP surface using a crank. The x-position can be adjusted manually to align the center of the coil with the center of the WP. To achieve movement in the y-direction, a DC motor, Figure 21a, is utilized and controlled by the standard control box, Figure 21b. The y-speed of the table can be regulated by adjusting a variable DC power

supply; however, there was constraint in terms of y-direction movement, Figure 23 shows maximum travel distance in y-direction for the table.



Figure 20 Pencil machine for the testing of the coils



Figure 21 a) DC motor for movement in y direction b) control box

Such set up let the coil to be fixed in stationary position, and the WP would be fixed on the moving table and by that, imitation of end milling is done. The feed rate of the WP, speed of table movement in our case, can be controlled by adjusting of the current, and a PLC system, the maximum speed was at the maximum value of the current,

which was equal to 24V, Figure 22. Such a set up lets us move under different speeds and different directions, giving the possibility to have 3D motion, and a range of imitation with adopting it to IAM verification.

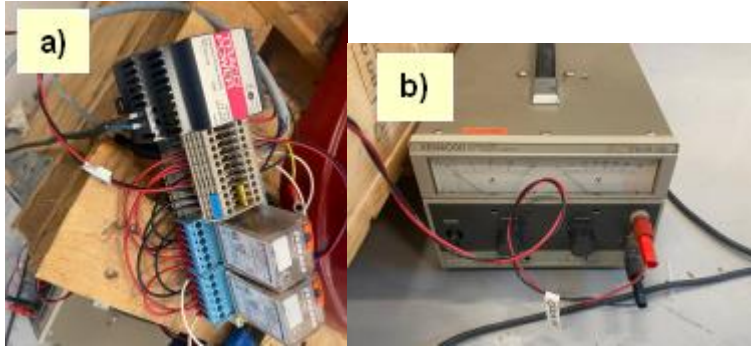


Figure 22 a) PLC b) current control device



Figure 23 Travelling range of the table in y-directions.

3.3. Thermal measurements equipment

For the measurement of the WP temperatures and visualization of the heating pattern FLIR ThermoCAM T360 was used, Figure 24. The IR camera is able to catch the range of temperatures from -20°C up to 1200°C , which is sufficient for our desired temperatures.



Figure 24 FLIR ThermoCAM T360

WPs were prepared in the form of rectangular slabs with dimensions of 290x82x27mm, Figure 25. To measure the temperature K-type thermocouples were glued on it with high temperature resistant cement. Additionally some thermocouples were placed underneath the WP to measure the bottom temperatures and temperature penetration and then were painted with black high temperature resistant paint, Figure 26, it was used to make certain that WP would have constant and known emissivity($\epsilon=0.9$), with which IR can read more accurate temperatures . Thermocouples were placed on the centerline of the WP for the insulation of the WP from contact with cast iron table superwool fiber was put between the WP and the table.



Figure 25 Workpiece in form of rectangular slab



Figure 26 Master Spray Paint 600 °Svart



Figure 27 Prepared workpiece with glued thermocouples

4. Conducted experiments

Chapter will described conducted experiments with the produced equipment and WP properties would be provided. Some proves of the concept would be made.

4.1. Material measurements

Materials of the interest in this research are M1 manganese austenitic steel and reinforced version of it. Material density, thermal diffusivity, thermal conductivity and specific heat capacity were measured.

To define the density of the WP, buoyancy density measurement method was used, which gave for M1 7.73g/cm^3 and for the reinforced WP it gave 6.83g/cm^3 .

For the thermal measurements stainless steel 310 was chosen as reference material as it's thermal properties are very close to the materials that are to be measured. To prevent oxidation of the materials, LFA measurements were done in oxygen-free environment. High quality argon (purity of 99.97%) was used to replace the air inside the chamber. Liquid nitrogen was used for cooling of the system between laser shots. Figure 28 shows the results of the measuring for the materials. As the softening temperatures of these materials are about $600\text{-}700^\circ\text{C}$, thermal measurements were done for extended range up to 850°C .

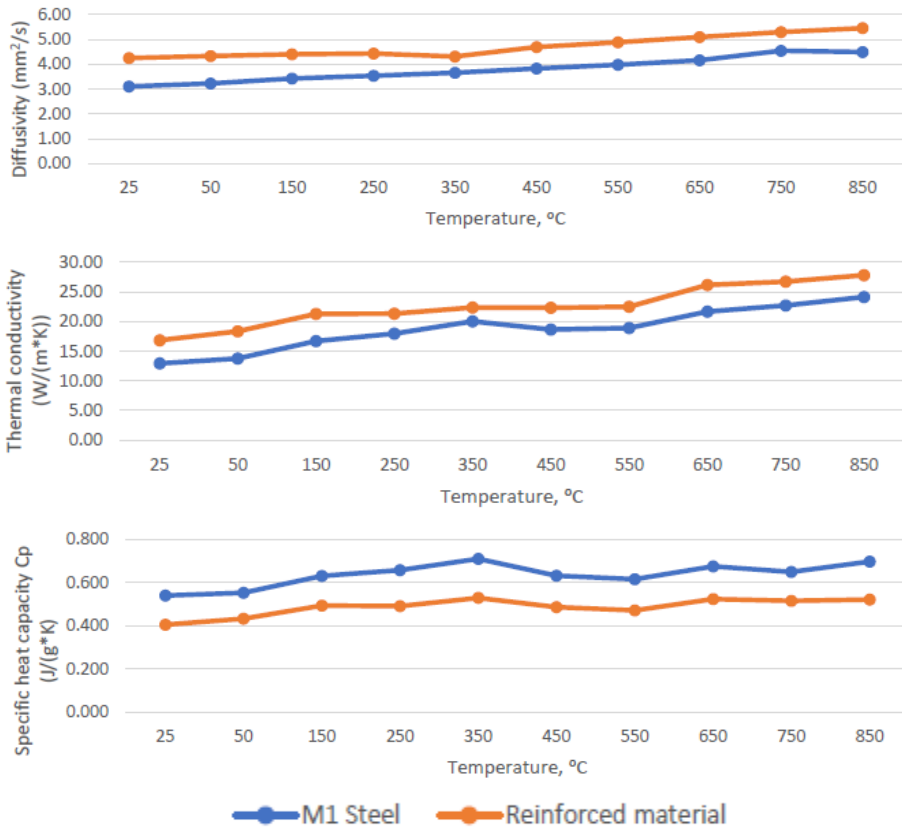


Figure 28 Measured thermal diffusivity, thermal conductivity and specific heat capacity of M1 steel and reinforced material

Measured tabulated data for both of materials can be found in Table 1.

M1 steel is a non magnetic material so it does not have any magnetic properties , same can be said about reinforced material.

C	Si	Mn	P	S	Cr	Ni	Mo	V	Cu	Al	Ti	Co	Nb	N	Fe
1.22	0.55	14.36	0.05	0.00	1.29	0.10	0.04	0.02	0.10	0.03	0.11	0.04	0.01	0.01	82.07

Figure 29 Chemical composition of M1 steel

Table 1 Tabulated data as function of temperature for the tested materials

Material	Temperature (°C)	Diffusivity (mm ² /s)	Conductivity (W/(m*K))	Heat capacity (J/(g*K))	Density (g/cm ³)
M1	25	3.11	12.95	0.539	7.73
	50	3.23	13.78	0.552	
	150	3.43	16.70	0.630	
	250	3.54	17.97	0.657	
	350	3.66	20.05	0.709	
	450	3.83	18.66	0.631	
	550	3.98	18.92	0.615	
	650	4.16	21.67	0.674	
	750	4.54	22.74	0.648	
	850	4.49	24.16	0.696	
Reinforced	25	4.25	16.87	0.404	6.83
	50	4.33	18.37	0.432	
	150	4.40	21.32	0.493	
	250	4.43	21.33	0.490	
	350	4.31	22.38	0.528	
	450	4.69	22.36	0.485	
	550	4.88	22.53	0.470	
	650	5.09	26.18	0.523	
	750	5.29	26.74	0.514	
	850	5.45	27.84	0.520	

4.2. Low frequency IAM imitation

For initial testing low frequency coil was used, it was done to testify the possibility of heating up the material and defining the nature of the heat spread on the material under most simple configuration.

Experiments were done from the highest speed of the 600 mm/min and then gradually decreased to 400 and 200 mm/min relatively, with long pauses in between experiments to cool down the material. As for the highest speed, reached temperatures would be lower which in the end will require less time for cooling. The measurements taken from thermocouples during the operation of the low frequency induction heater are presented in Figure 31. The data obtained from both the thermocouples and the IR camera show similar results, indicating the reliability of the temperature measurement using the IR camera. It is noteworthy that the peak temperatures were observed on thermocouple

ch4, whereas the lowest temperatures were recorded on thermocouple ch2, regardless of the speed of the process. This observation was further confirmed by the explanation that thermocouple ch4 had the best contact with the WP, while thermocouple ch2 had the poorest contact due to the thickness of the cement used to attach them to the WP.



Figure 30 Fully assembled testing equipment (Low frequency heating unit)

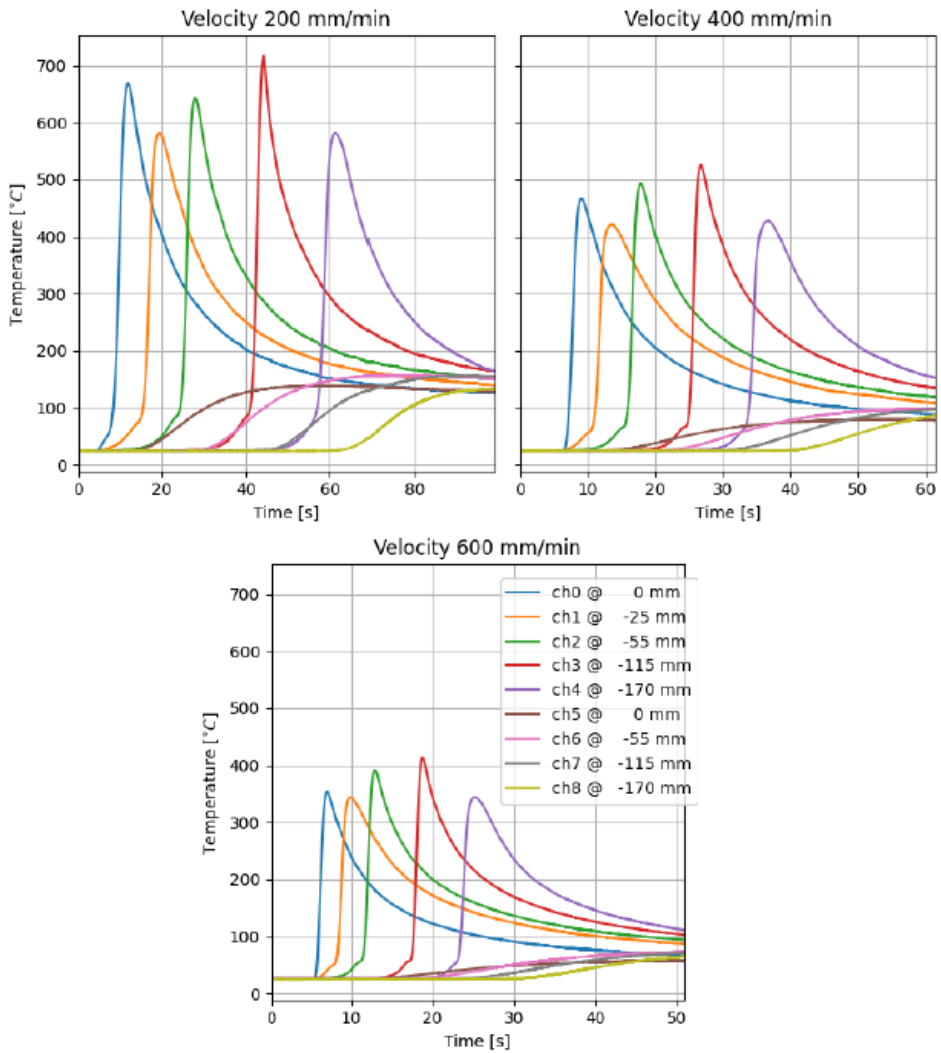


Figure 31 Measured temperatures by thermocouples. ch0- ch4 corresponds to the thermocouples placed on the surface, while ch5-ch8 are the ones on the bottom.

Using the low frequency induction coil showed us good results in terms of reached temperatures. The reached temperatures at a lowest speed was about 600°C, which is a lower limit for the required temperatures, as from this point significant drop in Mn-steels hardness starts.

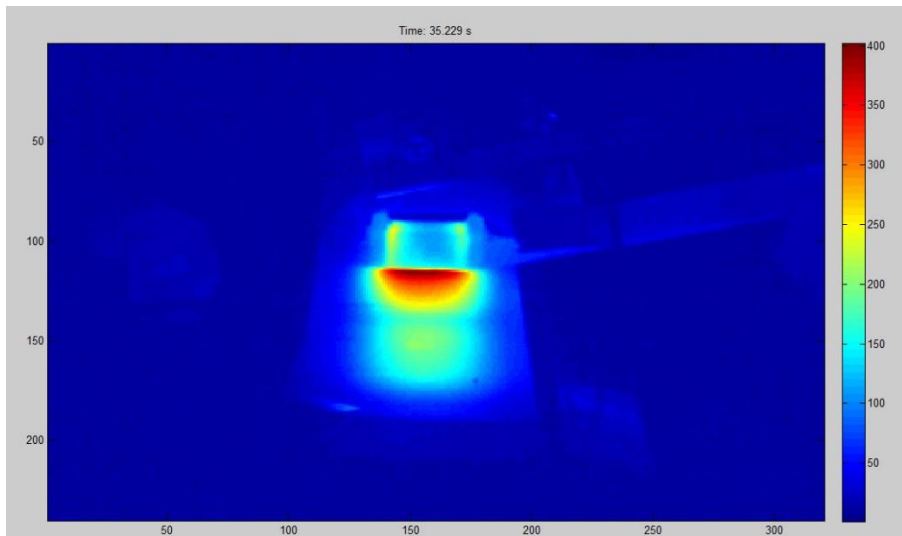


Figure 32 Heat pattern of low frequency heating unit, under the speed of 600mm/min

The use of a low frequency (16.7 kHz) induction heater results in higher heat generation within the bulk of the paramagnetic manganese steel M1 material manufactured by Sandvik SRP. However, this effect becomes more pronounced at lower speeds. Figure 32 shows us a heating pattern and the reached temperatures captured by IR camera, at the speed of 600mm/min.

It is clearly seen that heated area is very wide, which is not actually needed for the actual machining as the contact area of the tool and the WP would not be that wide in the scope of turning. In scope of milling such, big heated area is acceptable, but the depth of the heat still very deep and for the milling more concentrated heat close to surface is needed.

In overall depth of heat was very deep, from the measurements in Figure 31, heat penetrated the full depth of the WP and even on the bottom part temperatures reached about 150°C, which means upper layers were even hotter and it lead to deterioration of the material, which further will result in much worse machining conditions. Also should be said that such deep penetration is wasting of power output, which would be more efficient if concentrated on the depth of an actual cut, which will gather faster heating but on the lower depth. To address this issue, a higher excitation frequency is recommended, as this would

confine the smaller skin depth closer to the surface, and will be described further.

4.3. High frequency milling coil

With intent to be used in milling, custom-made coil was designed and produced, Figure 33- Figure 35. As it intended to be used for the milling and engagement area with the WP is planned to be about 43mm, coil length was made for exact same width.

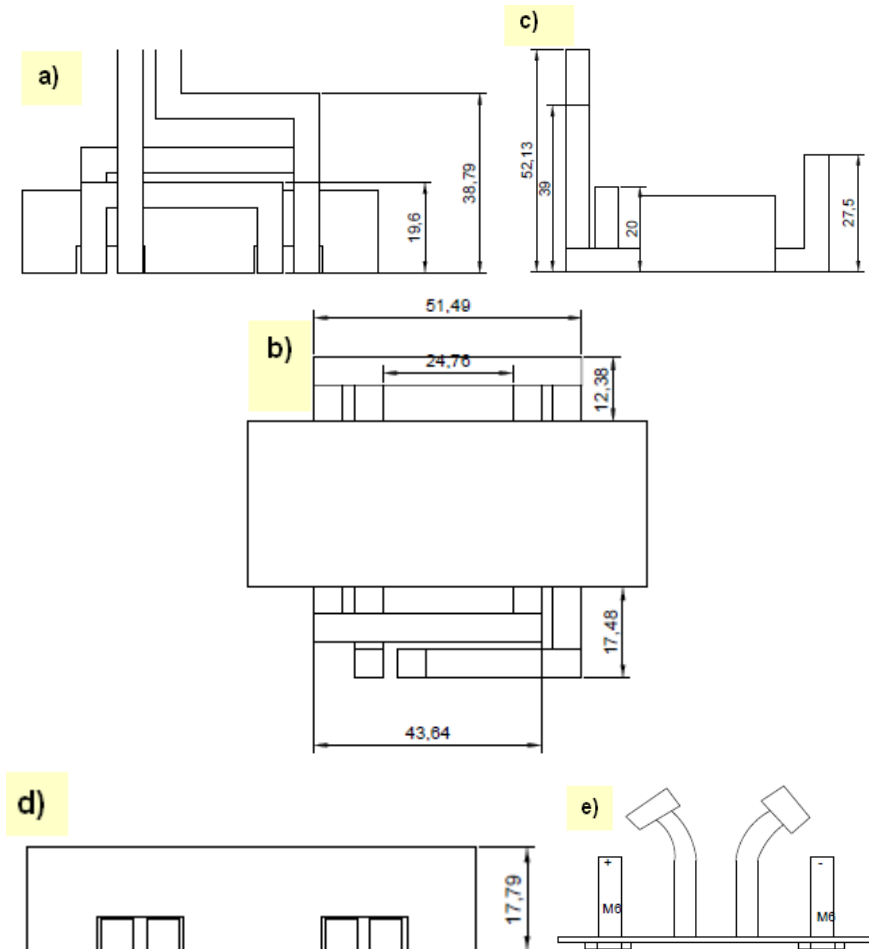


Figure 33 Draft version of the HF milling coil design. a) Front view, b) Up view, c) Side view, d) section view, e) power source connectors , and water- in -out adapters

Design of the coil was done in accordance with the size of the WP, tubes were supposed to be bended up, to eliminate the problem of excessive flux generation out of the ferrite covering area.

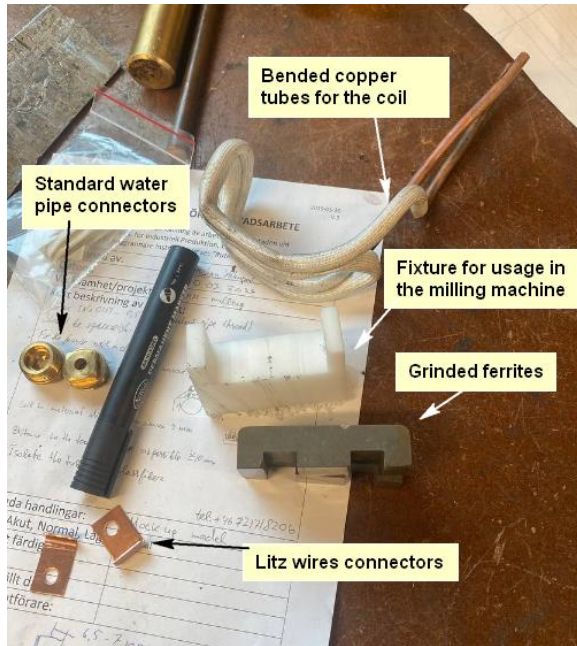


Figure 34 Separate parts for the milling coil

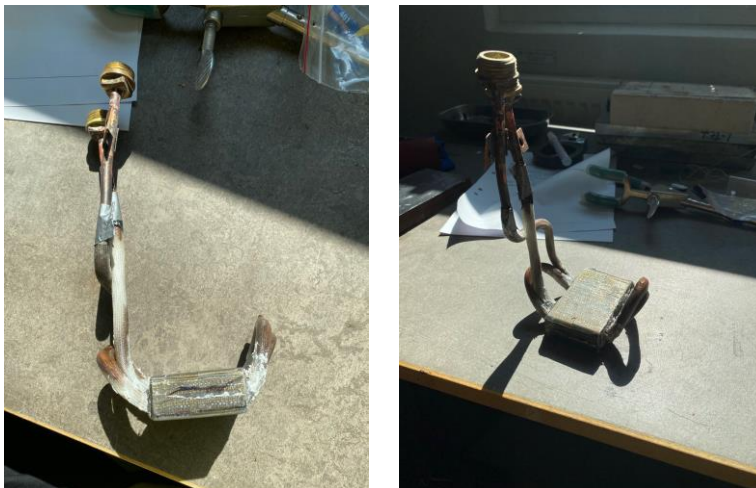


Figure 35 High frequency coil for milling

Coil was produced with some correction, for more ergonomic design and simplicity to mount it into milling machine. After all of the parts were produced, ferrites were fixed by the use of the epoxy resin, for firm contact with a ferrite and to avoid dissembling of the parts during actual use of it.

The coil was used with an induction frequency inverter that was capable for maximum power output of 15 kW, Figure 36.



Figure 36 Induction frequency inverter

The whole set up can be seen in Figure 37.

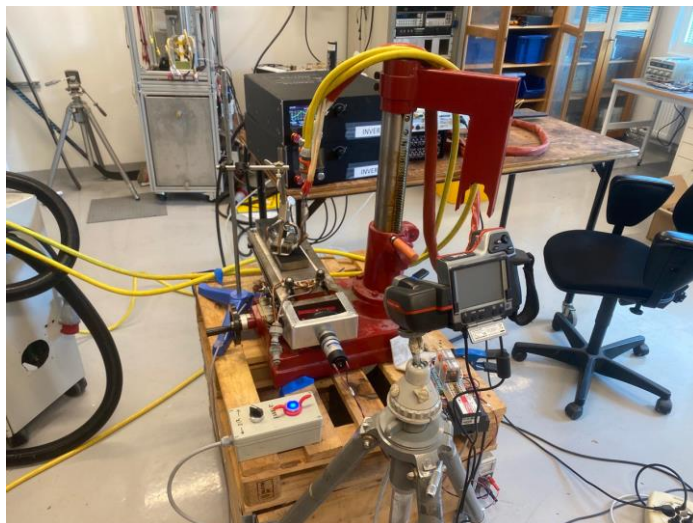


Figure 37 Set up for the milling coil testing

Working range of inverter frequencies in this set up was from 100kHz to 1000kHz. Inverter itself had a sweep function, which helps to find resonance frequencies for the coil, and after adjusting, resonance frequencies were 300 kHz-330 kHz.

Testing of all configurations was done with the maximum speed of 1143 mm/min, as it is the maximum speed of the pencil machine and milling is assumed to be done relatively close to this value.

To prevent set up from damage and to observe the behavior of the coil under different power inputs, range of different current as the main input was tested, starting from the 15A ending with 40A which supposed to give the highest power output and generate the highest temperatures. In the following figures heat pattern under different power inputs can be observed, the scale on the right side of the figures shows temperature of the heat pattern, which can be defined by color.

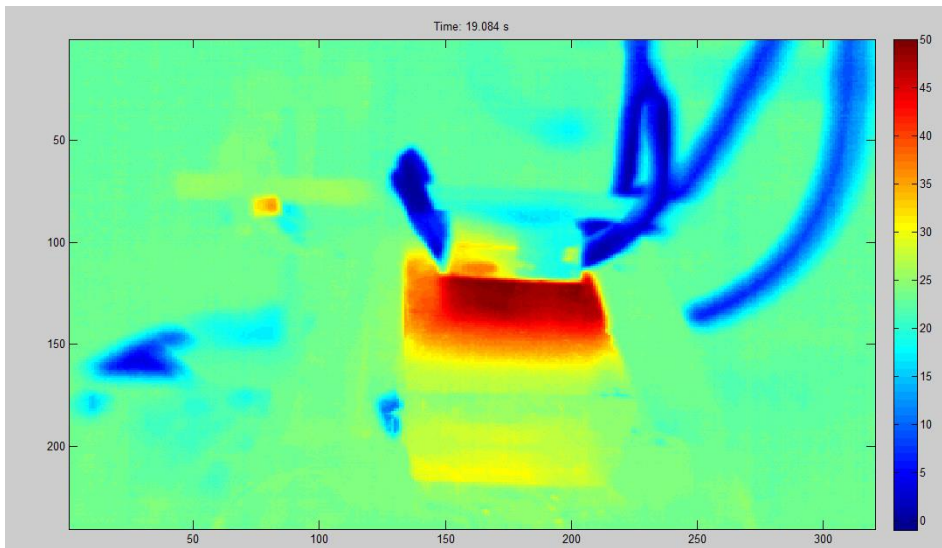


Figure 38 Heat pattern, under the current of 15A

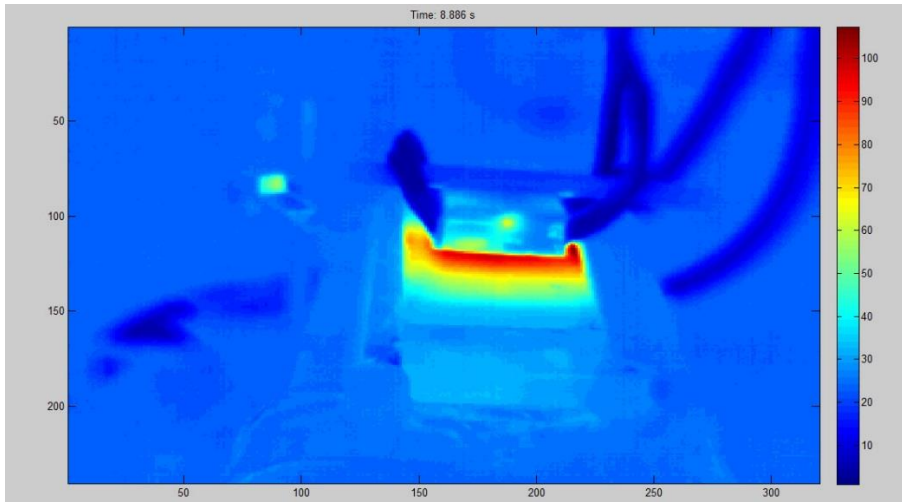


Figure 39 Heat pattern, under the current of 18A

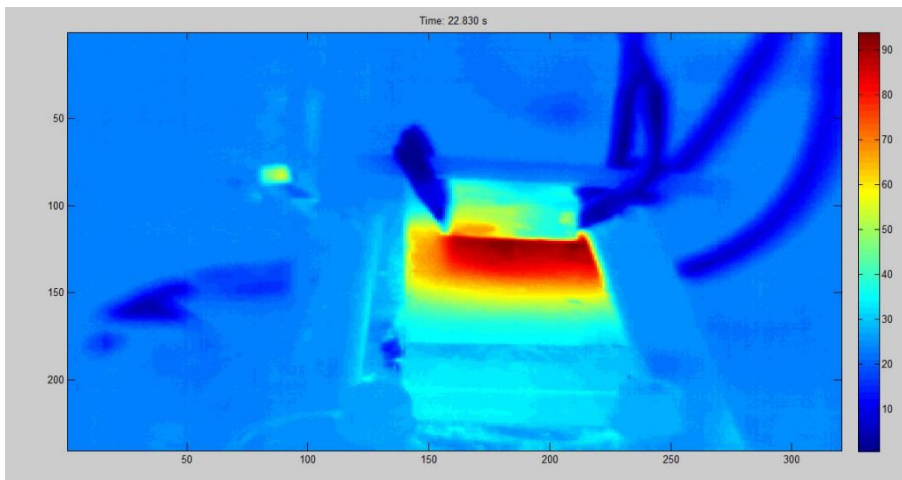


Figure 40 Heat pattern, under the current of 20A

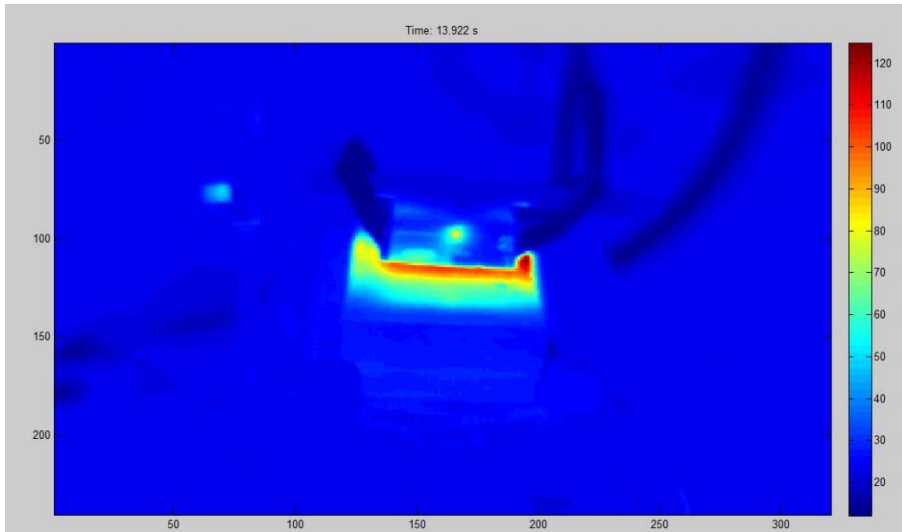


Figure 41 Heat pattern, under the current of 25A

From the Figure 41, we can see that maximum temperature that was reached are not sufficient enough to soften the material, and the power output that was gained was 8-9kW, which in theory should give use relatively high heat generation on the WP material.

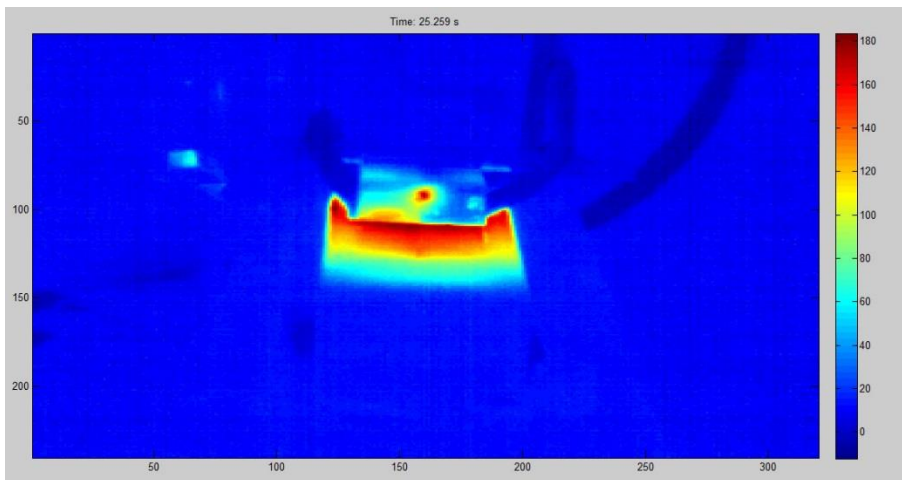


Figure 42 Heat pattern, under the current of 35A

Under the current of 35A we can observe heat generation in the ferrite itself, Figure 42, which leads to the decrease in its functionality, because under higher temperatures ferrites loses efficiency in terms of

flux concentration, and its main purpose was to concentrate the magnetic flux on the WP. Under the current of 35A, power output was 11-12kW and the maximum WP temperatures reached 200°C. Should be mentioned that power output that is shown on the inverter interface does not really reflect an actual power transferred on the WP.

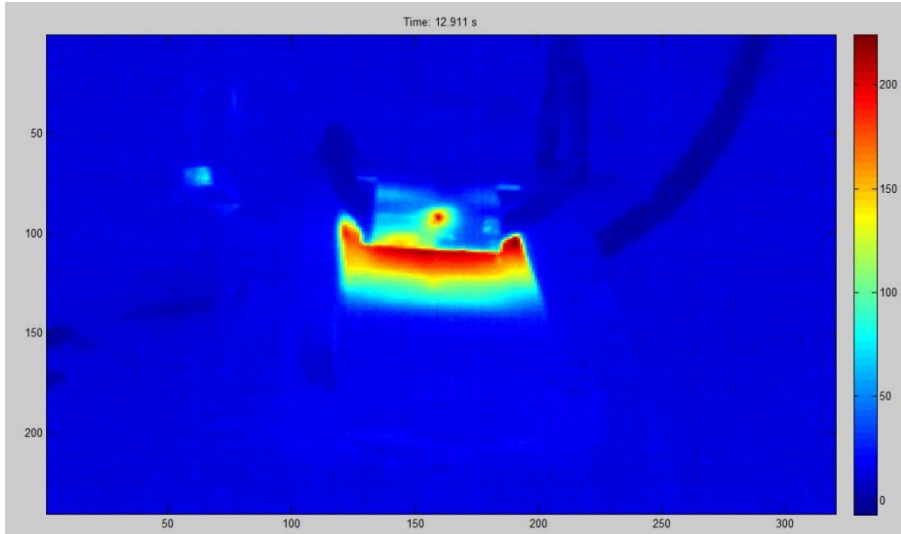


Figure 43 Heat pattern, under the current of 38A

Under the current of 38A, displayed power output was 12-13kW, which in theory should give us enough heat generation, but the maximum temperatures that were reached are just 260°C.

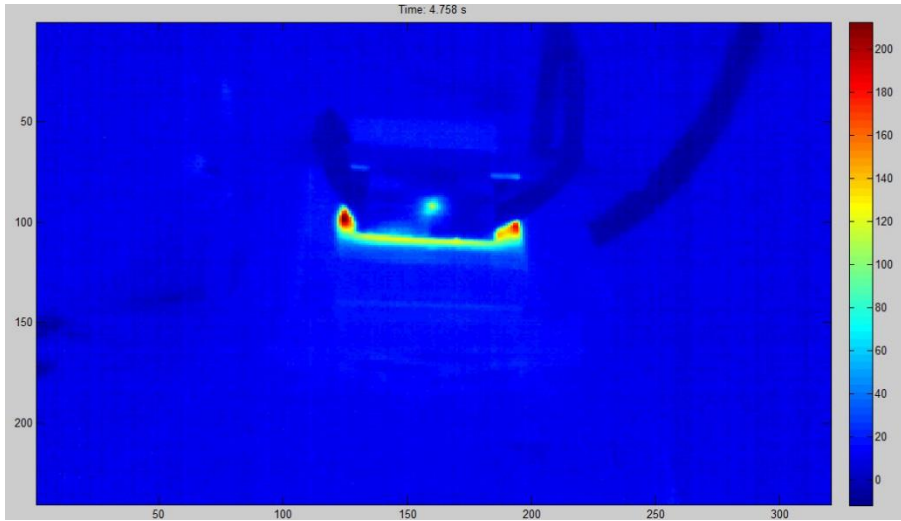


Figure 44 Heat pattern, under the current of 40A

Preliminary high frequency milling coil testing, showed that current set up is not sufficient enough as the material was not heated to the minimum required temperatures. According to the figures in this subchapter, it can be assumed that ferrite was overheated, and reached its Currie temperatures, and under such temperatures ferrite loses its ability to concentrate the magnetic fluxes, and they penetrate it, which in the end gives high percentage of loses as the flux is not concentrated on the WP.

4.4. High frequency turning coil

For the turning processes, much narrowed heating area should be considered as the amount of the material to be removed for one turn is much lower in comparison with milling, the heated area of about 1mm^2 would sufficient.

The device shown in Figure 45 incorporates a flux concentrator made of ferrite to enhance efficiency and power density by eliminating the magnetic field within the heater itself, device was also used with a same induction frequencies inverter as in initial testing of the milling coil, Figure 36 . A copper shielding, 3D printed to form a one-turn coil, which concentrates the flux in a narrowed region for faster and more efficient heating. The copper shielding features internal cooling tubes

to maintain suitable permeability and prevent drops in magnetic flux with rising temperatures. The ferrite is installed within the copper shielding using copper paste for improved heat transfer and pressed against the copper shielding using fiberwool for better thermal insulation. The lid is covered with Kapton film for electrical isolation and to withstand the high temperatures generated during use. Additionally, a temperature sensor (PT100) is employed to measure internal temperatures of the heating unit.



Figure 45 High frequency coil for turning

For the testing of the M1 steel the heating unit was wound using 12 turns of litz wire. The testing involved applying currents ranging from 8A to 18A. However, when a current of 18A was used, excessively high temperatures were observed on the lid, as depicted in the accompanying Figure 46.



Figure 46 Point of the highest temperatures in the heating unit

During testing, heat generation was observed on the lid portion of the heating unit, as illustrated in Figure 46. This was particularly noticeable when a current of 18A was used, Figure 47, as the flux concentration was highest at the middle bottom portion, resulting in the highest temperatures in that region. Consequently, a decision was made to enhance the cooling system in order to proceed with further testing.

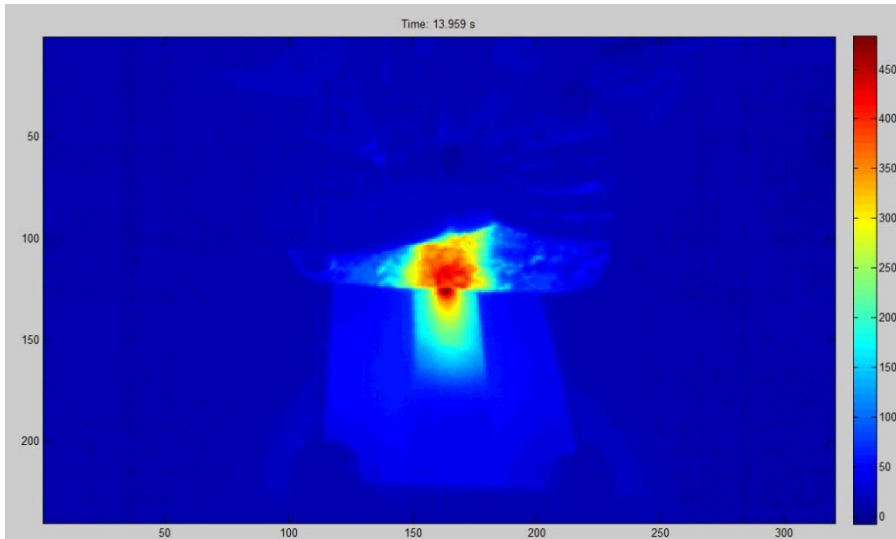
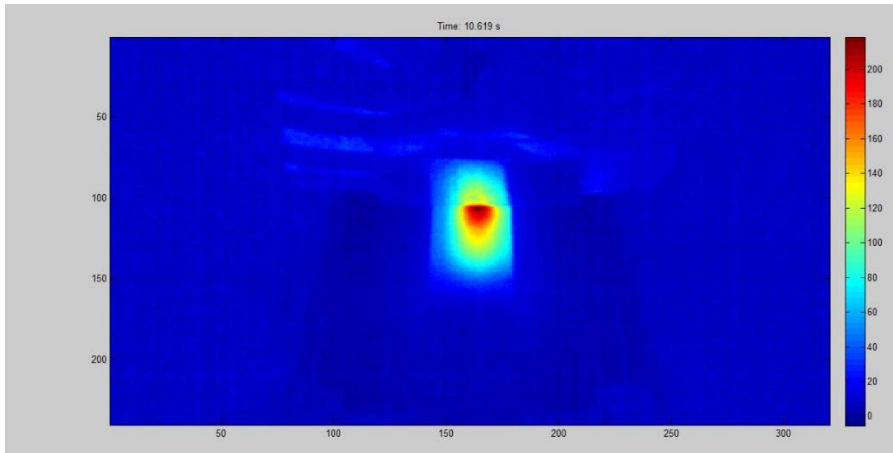


Figure 47 $V_c=1000\text{mm/min}$, Current 18A

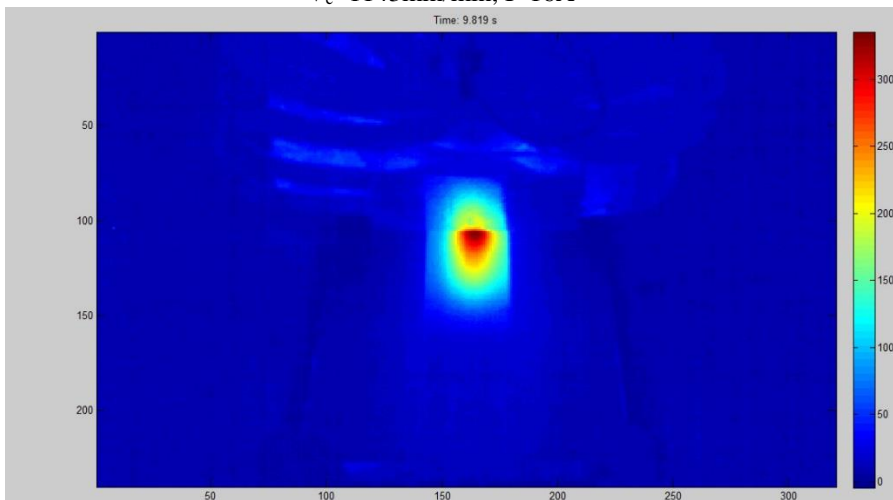


Figure 48 Cooling added to the lid

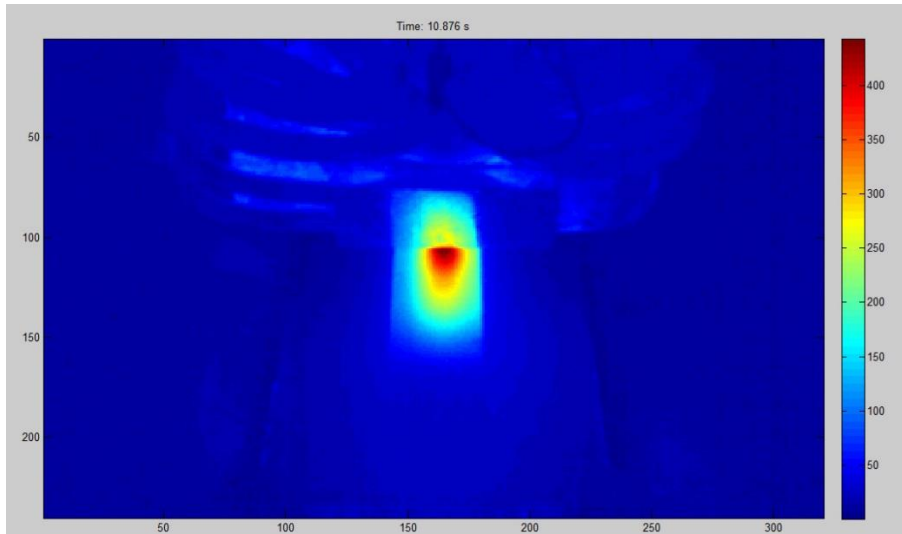
Subsequent testing was conducted within a current range of 8A to 28A, corresponding to a power output of approximately 4kW to 12kW. However, at peak power outputs, the cooling system proved insufficient, causing the water used for cooling to boil and resulting in an overall reduction in cooling efficiency. Despite this, the temperatures attained during testing were deemed sufficient for machining purposes, with maximum temperatures reaching up to 600 °C at a speed of 1143mm/min.



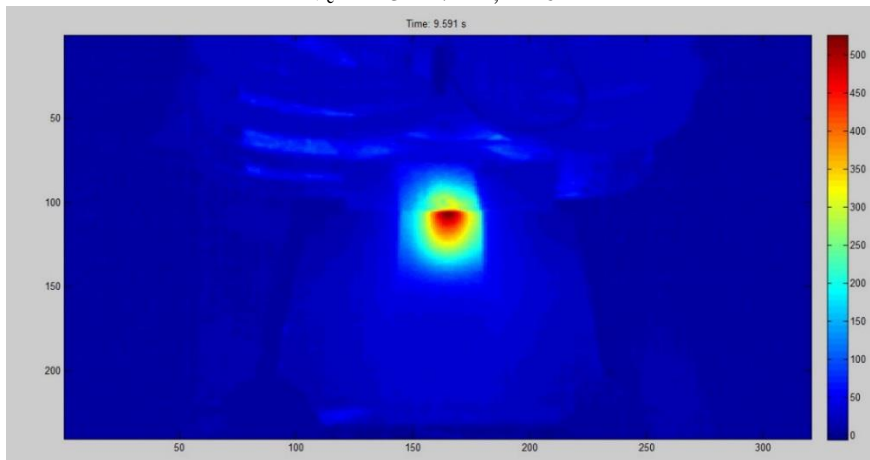
$V_c=1143\text{mm/min}$, $I=16\text{A}$



$V_c=1143\text{mm/min}$, $I=22\text{A}$



$V_c=1143\text{mm/min}, I=26\text{A}$



$V_c=1143\text{mm/min}, I=28\text{A}$

Figure 49 Experiments with added cooling system to the lid

From Figure 49, under the current of 28 A we reached minimum limit of the temperatures required for the actual machining processes, which proves efficiency of the coil and gives us possibility for actual machining of the material.

4.5. Analysis of conducted experiments

Conducted experiments showed efficiency of the turning coil and further actual in machine testing can be performed.

During testing of the high frequency (HF) turning induction coil, possibility to reach desired minimum was proven, which gave clear understanding that further testing in the lathe can be conducted. Under the lower limit of the temperature that was reached, one of the tested WP had a melted pattern that proves softening of the material, Figure 50

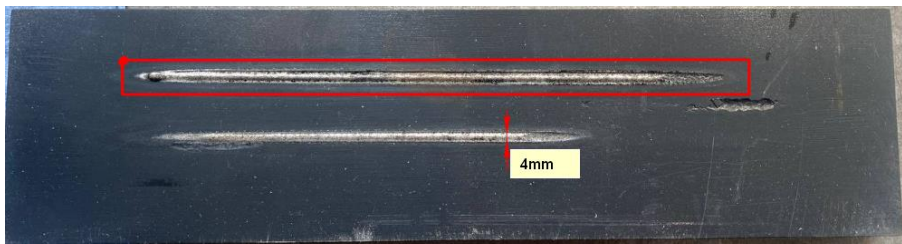


Figure 50 Melted path

From Figure 50 it is clearly seen that only desired area was heated, and the concentration of the magnetic fluxes was exactly at the desired width and depth, which responds to the requirements of the turning cutting input data.

For the milling, coil's further adjustments such as cooling system for the ferrite, usable frequencies range and inverter set up should be considered.

It may appear to be a relatively straightforward procedure that involves utilizing the total consumed heating power, as the control input. In this context, the voltage applied to the induction coil can be viewed as the necessary control function. However, the control process becomes more complex due to the challenges associated with achieving the desired spatial distribution of internal heat sources. It may be difficult or impractical to attain a specific power distribution along the length of the induction coil. Many existing methods for controlling power distribution face significant limitations or are unable to generate the required spatial distribution of internal heat sources when heating certain metals (Faulkner, 2007).

When using adjustable frequency supplies, it is possible to consider frequency as a control input parameter that influences the spatial distribution of internal heat sources. By controlling the depth of the subsurface heat-generating layer over time, referred to as variable current penetration depth, the spatial distribution can be managed (Faulkner, 2007).

The first group of control inputs consists of parameters that are not dependent on space coordinates. These control inputs are time-dependent parameters, known as lumped control inputs, and include voltage, current, or frequency of the operating current, power of each coil, and production rate of progressive multistage heaters or speed of continuous heating installations (Faulkner, 2007).

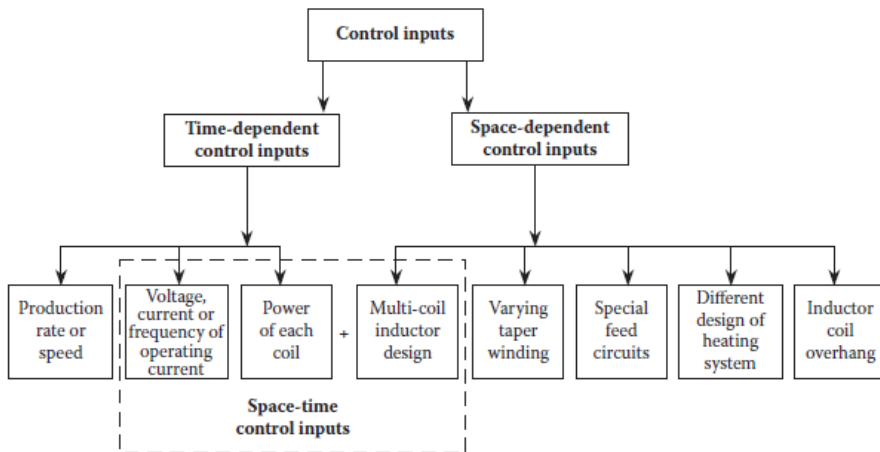


Figure 51 Control inputs used for induction heating processes (Faulkner, 2007)

These control inputs align with the notion that "control input" involves specific "steering wheels," with their operating positions being modifiable over time in a desirable manner. Another effective way to control heat sources is through coil power. By appropriately varying the coil voltage, this control input can be easily manipulated. It is important to note that coil power is proportional to the square of voltage, hence the power density of electromagnetic heat sources, can serve as a convenient time-dependent control function commonly used in induction heating processes (Faulkner, 2007).

The choice of operating frequency can also be viewed as an alternative control input. However, the requirement for adjustable

frequency in the power supply may introduce unwanted system complexity and additional costs (Faulkner, 2007).

5. Iterations in the design and use of the coils

Adjustments for the milling set up are done in this chapter, with an attempt to solve the problems which occurred previously. Imitation of the IAM in turning lathe is performed.

5.1. Milling coil issues and modifications

Milling coil did not show any sufficient results during the initial experiments. Most probably, it was connected with impedance matching and by the current invertors configuration there is no possibility to achieve the desired result. Impedance matching for the coil is very important as the induction heating process, which involves the transfer of energy from an alternating current (AC) power supply to a WP via electromagnetic induction.

Based on the section 4.5 some of the following adjustments to the set up was done. In induction heating, a coil is used to create a magnetic field, which induces eddy currents within the WP, causing it to heat up. To ensure efficient and effective heating, the impedance of the coil and the WP must be matched.

Impedance is the resistance that an electrical circuit presents to an alternating current. When the impedance of the coil and the WP are mismatched, it can lead to inefficient power transfer and overheating of the equipment.

To achieve impedance matching, the coil's inductance and the WP's capacitance are adjusted. This can be done by adding or removing capacitors. Once the impedance of the coil and the WP are matched, the maximum amount of power can be transferred to the WP, resulting in efficient and effective heating.

By adding or removing capacitors in parallel or series with the coil, the total impedance of the circuit can be adjusted to match the impedance of the WP.

In other words, if the WP has a high reactance, a capacitor with an appropriate value can be added in parallel with the coil to cancel out the reactance and achieve impedance matching. Conversely, if the WP

has a low reactance, a capacitor can be added in series with the coil to increase the circuit's total reactance and achieve impedance matching.

Achieving impedance matching is crucial for the induction heating process to be efficient and effective. Capacitors can be used to fine-tune the impedance of the system, ensuring maximum power transfer to the WP and avoiding overheating of the equipment.

So with accordance that was told above decision to swap to the parallel connection of the capacitors and in series to the coil was done, also two transformers were added in parallel so the current that goes out would be high for more efficient power transferring to the WP.

First set up was done with 9 paralleled capacitors, each was $0.1 \mu\text{F}$, of paralleled capacitors and with two transformers. Under such configuration corresponding frequencies (500-700 kHz) were too high which gave us oversaturation of the ferrite, and disabled the use of it.

Next set up was with 4 paralleled capacitors with values of $0.33 \mu\text{F}$ – 2 pieces and $0.25 \mu\text{F}$ – 2 pieces, which were connected in series to the coil, Figure 52. In this set up, two transformers parallel connected, and we were not able to reach highest power output of the inverter due to over current error during exploitation process.

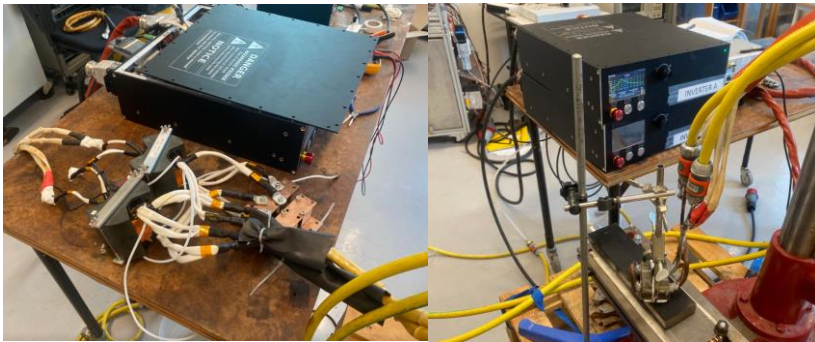


Figure 52 Milling coil testing set up



Figure 53 Paralleled capacitors and transformers and as the series to coil

Next modification for inverter set up was to parallel connect one more transformer which in the end suppose to give us higher power output with lower current input, and should give better impedance matching. In addition to offload heat generation on the ferrite, cooling cover for the ferrite was designed, Figure 54.

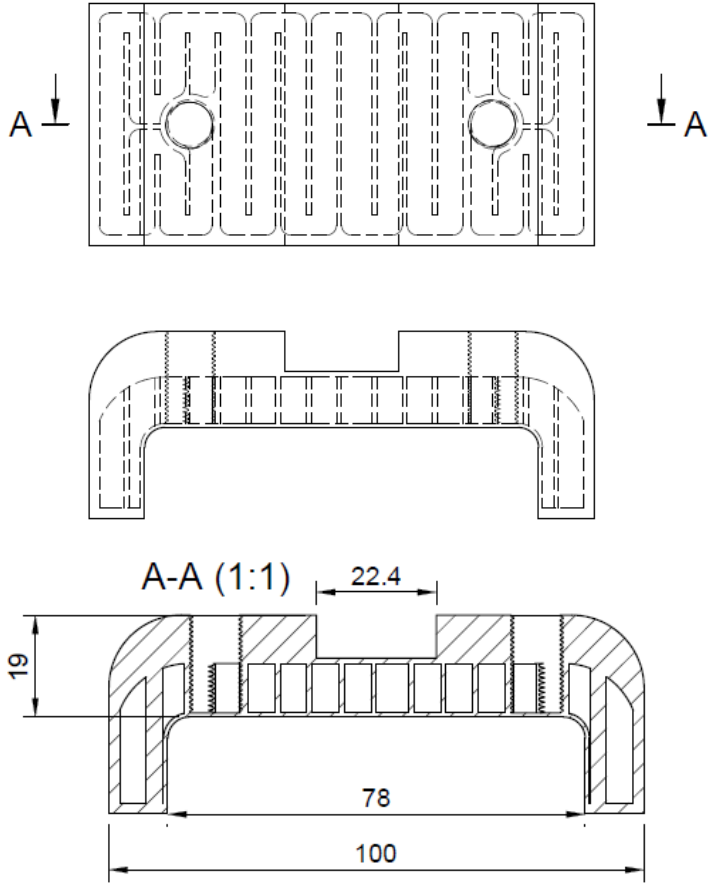


Figure 54 Design of the cooler for the ferrite



Figure 55 3D printed ferrite cooler

After all of the modifications that were done, sweep was done and resonance frequencies were settled, 239kHz – 265kHz.

Under current configuration we were able to reach higher temperatures than in original set up. Moreover maximum power output was reached under lower currents.

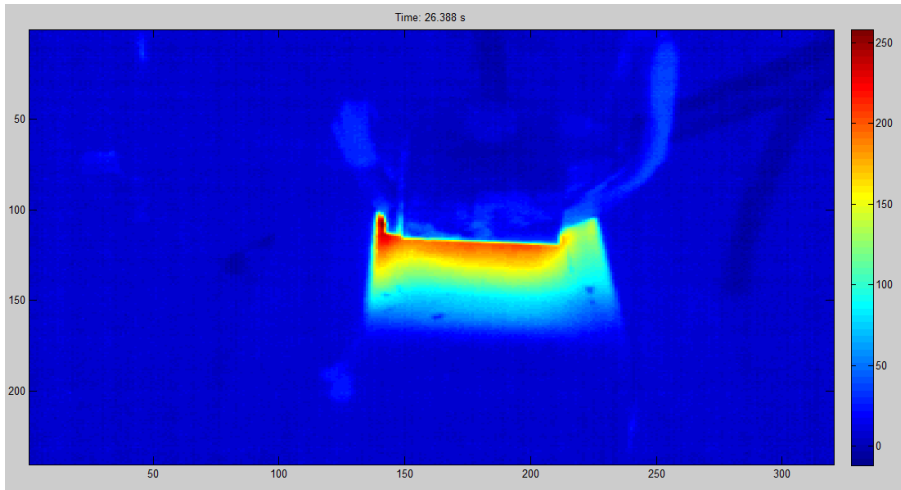


Figure 56 Current of 25A, power output 10kW, maximum temperatures of the workpiece 260-270°C

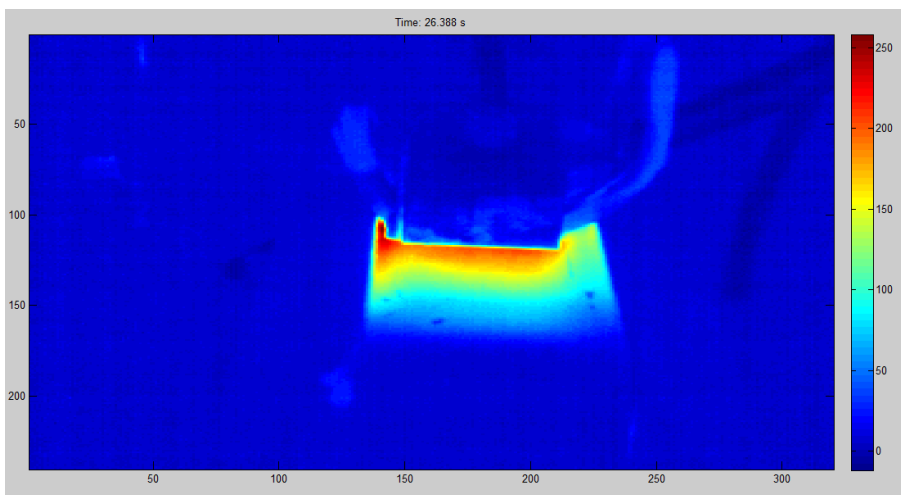


Figure 57 Current of 27A, power output 12kW, maximum temperatures of the workpiece 290-300°C

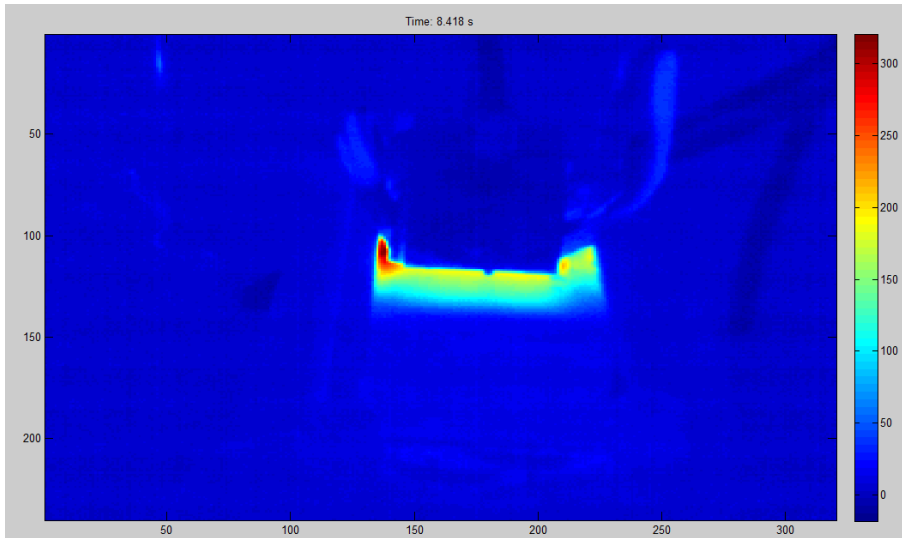


Figure 58 Current of 29A, power output 14kW, maximum temperatures of the workpiece 320-330°C

Even with the modified set up we were not able to reach desired temperatures, which can be seen in Figure 58, even though the heated area and heat penetration is suitable for milling, but main criteria which is a temperature was not reached with a current set up of the coil. With the decrease in feed rate to 0.6m/min, the peak temperature can be seen in Figure 59. With a longer induction time desired surface temperature also was not reached.

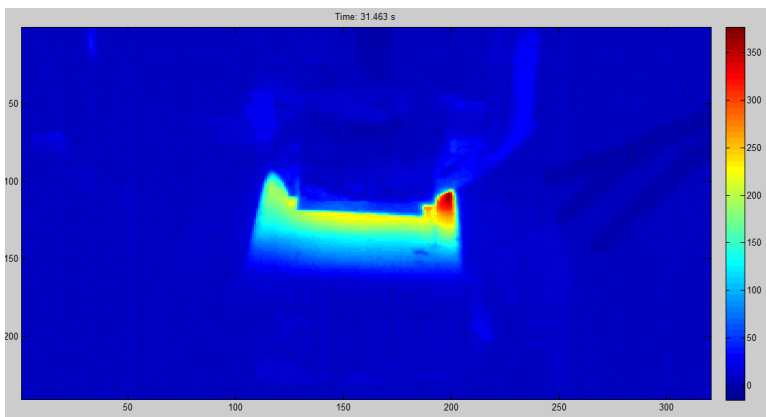


Figure 59 Current of 29A, power output 14kW, feed rate 0.6 m/min, maximum temperatures of the workpiece 380°C-400°C

5.2. Experimental validation of high frequency induction coil for turning

Experimental validation of high frequency turning coil will be conducted in the SMT turning machine, Figure 60.



Figure 60 SMT turning lathe



Figure 61 Workpiece mounted into lathe

WP was mounted into lathe and painted with heat resistant black paint, for a better IR image capturing.

Design concept was done for the HF turning coil holder, for fixturing it into SMT lathe, Figure 62.

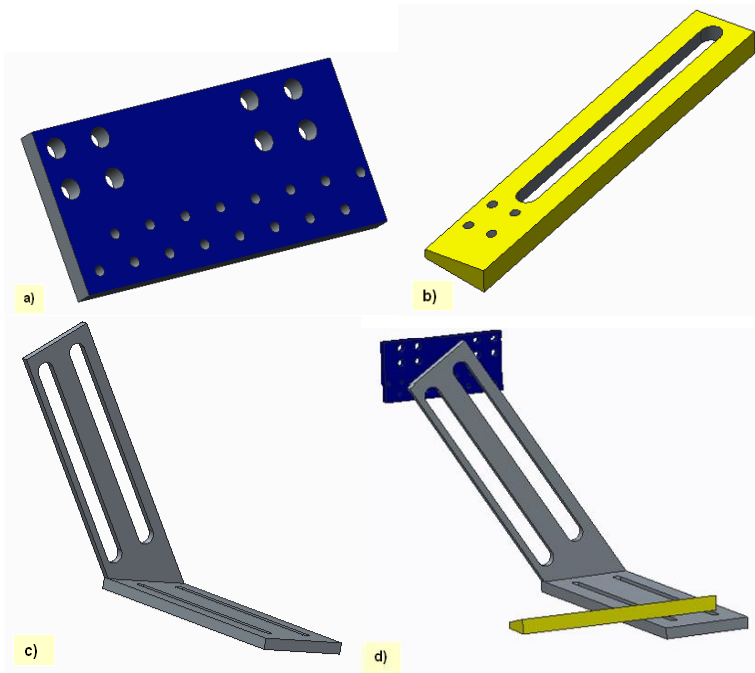


Figure 62 Conceptual design for the HF coil holder. a) Attachment to the SMT machine. b) Rack for coil fixturing attachment and axial distance control. c) Rack for the perpendicular take out of the coil, to avoid collision with the tool. d) Assembled version.

Holder for the HF induction turning coil was manufactured for a better control of the distance to the WP, Figure 63. Original design was changed, according to the workshop staff experience, to make the holder stiffer and easier to manufacture. Main criteria for the holder was to make it controllable in all directions, and it also should withstand the weight of the coil, so actually produced holder is thicker to avoid bending of the rack and to withstand vibration that can occur during the machining.

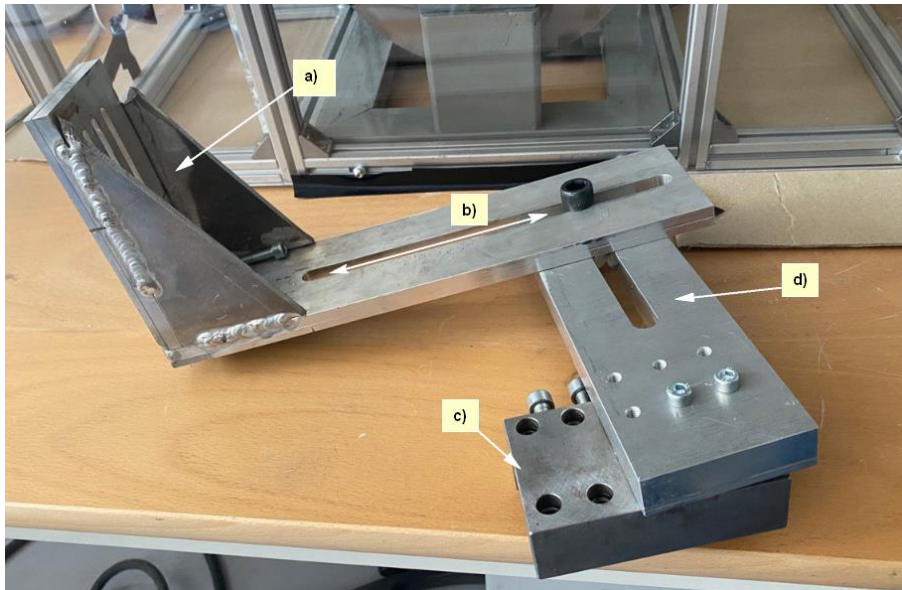


Figure 63 Holder for the HF turning induction coil. a) Is attached to the SMT tool holder, for the movement along with the tool. b) Hole is made to control the distance of the coil to the workpiece. c) Coil fixturing, also possible to control the distance to the workpiece. d) Gives possibility to control distance of the coil in axial direction.

One power unit (Induction frequency inverter) with a maximum power of 15kW was used for testing of the coil performance in the SMT machine, to define maximum temperatures that can be reached with one heating unit.

Frequency that were used were in range of 200kHz-300kHz. Rotation speed of the work piece ($D=114\text{mm}$) was 260rpm.

Initial current that was chosen for testing was 30A, which corresponded to approximately 8kW of power output. Heat was generated in a matter of seconds but was low and did not suit required temperatures. Temperature of the WP that was reached was about 400-420 °C, Figure 64.

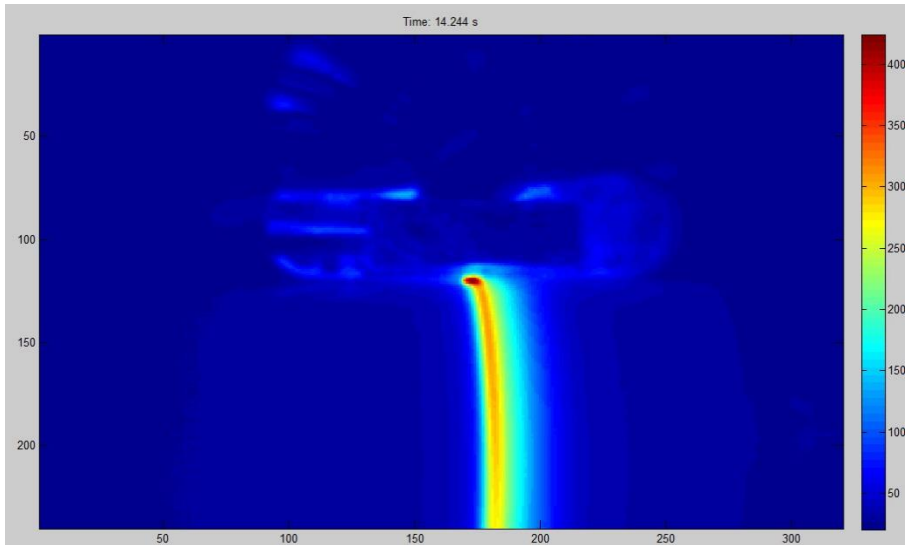


Figure 64 IR camera image, temperature pattern under the current of 30A

After increase in current values, more power was used for the heating process, about 9 kW, which did not give any sufficient results. We can see on the Figure 65 that temperature that was reached do not have significant difference with the previous values. Maximum reached temperatures also was about 400 °C. However, it was spread more uniformly on the WP surface.

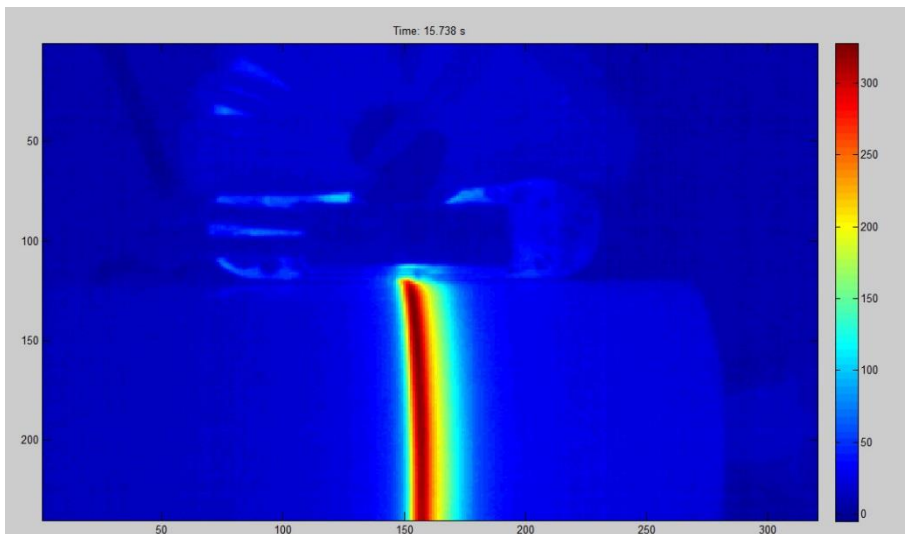


Figure 65 IR camera image, temperature pattern under the current of 32A

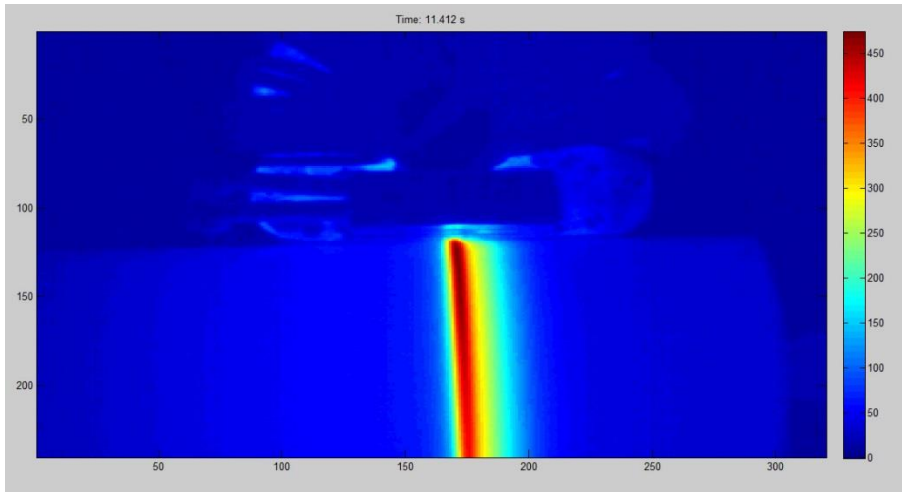


Figure 66 IR camera image, temperature pattern under the current of 40A

From Figure 66 we can see the heating pattern and the reached temperatures under maximum power output from one unit, which is 15kW. The maximum reached temperatures were in the range of 470-480°C.

Further step was to decrease the rotational speed of the WP to see if we can actually heat it to the lower limit of required temperatures, so rotational speed was decreased to 160rpm.

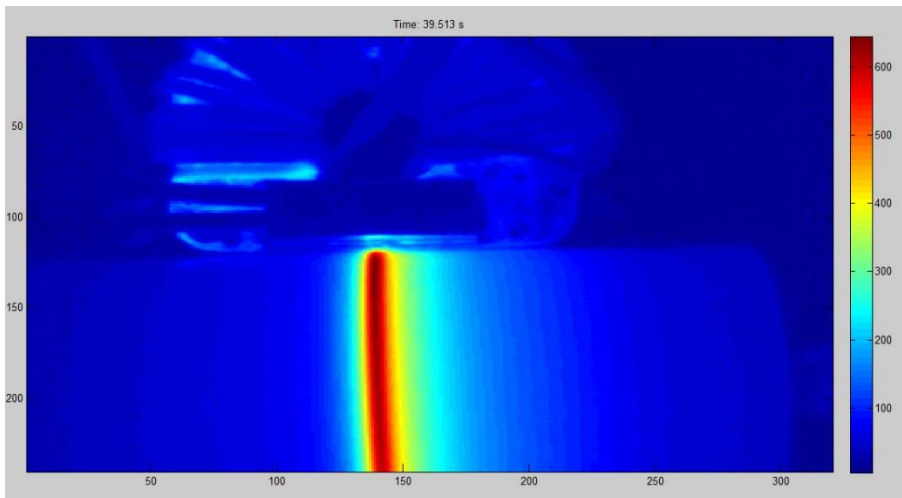


Figure 67 IR camera image, temperature pattern under the current of 40A, decreased rotational speed of 160rpm

From Figure 67 minimum temperature requirements were reached, in an actual experiment temperatures were 650°C-680°C. When we reached these temperatures, some other problems were faced. Cooling of the coil was not sufficient, and under such conditions continuously usage of the coil would not be possible. Another problem would be that under current power input and set up with one induction coil, we are not able to reach all desired range of temperatures. These problems could have appeared due to the cooling paste that was used (copper paste), as it has low thermal conductivity (4.68 W/mK).

After disassembling of the coil, ferrite part was investigated and some damage was seen on it.

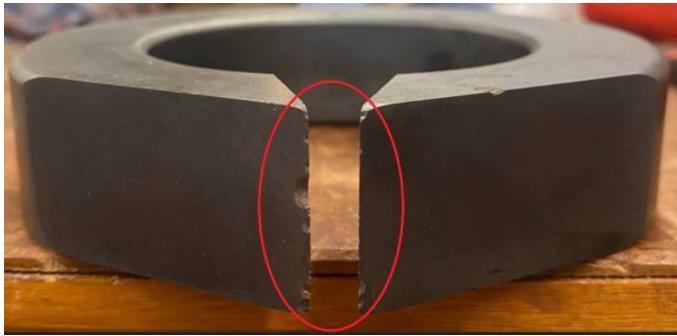


Figure 68 Damage on the tip of ferrite

Damage was probably been caused by the temperature due to insufficient cooling, which is expected. On the tip of the core, excessive temperature is usually formed, which will cause thermal expansion and by that, some micro damage can appear. Improve the cooling would be the next step for further testing. It would be also beneficial to go up in frequency to maintain the output power without saturating the ferrite core, despite the increased loss density. With more efficient cooling more power could be used as the temperatures involved in the coil would dissipate faster and performance in overall would be better.

For heat exchange improvement, another cooling paste was tested and showed good results, there was no overheating of the coil (cooling paste thermal conductivity was 11.5W/mK), which let the setup have a better heat exchange between the ferrite and a copper coverage.

To reach all of the desired temperatures range new set up with two power units was tested.

Two invertors were used, with purpose to increase the power, up to 30kW. Moreover, use higher frequencies to maintain the output power without saturating the ferrite core, despite the increased loss density. For the start minimum values were used to run the testing, the power of the 14kW was tested and everything went smooth. Frequencies were set to 511 kHz, current was set to 25 A for each unit which in total gave us about 17kW of power output. However, during the heating process it was not stabilizing which was not right for this process.

After different attempts were done to adopt the output to be stable and give a constant power generation and by that firm heat patter on the WP. During diagnosis process, smoke was noticed coming out from the inside of the coil, Figure 69.



Figure 69 Failure of the coil

Later coil was disassembled for inspection and identification of the damage. Disassembled coil can be seen in Figure 70.

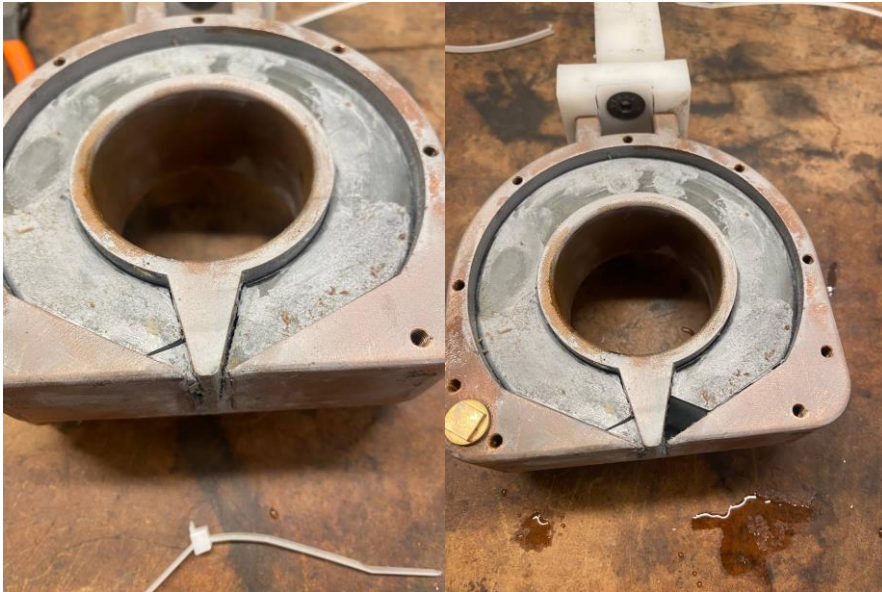


Figure 70 Core damage

From Figure 70 we can observe severe damage of the coil core, that was caused by over saturation of it and by that causing excessive temperatures. On the place where it cracked, it can also be that current went through ferrite to the inner part of the coil, which caused its destruction.

Should be said that on the outer surface of the coil and on the IR camera there were no excessive temperatures noticed. So most of the heat generation was on the tip of the core.

From conducted experiments conclusion can be made that for the one heating unit maximum suitable power unit would be 14kW, and suitable frequencies should be in the range of 300 kHz, which will not over saturate the core and will not destroy it further.

6. Results and discussions

Following chapter will describe some correlations and key factors for the process of induction heating that were observed during the project

From all the experiments that were conducted, there is a correlation with area of the heat, velocity of the WP or the coil itself to the behavior of the heating.

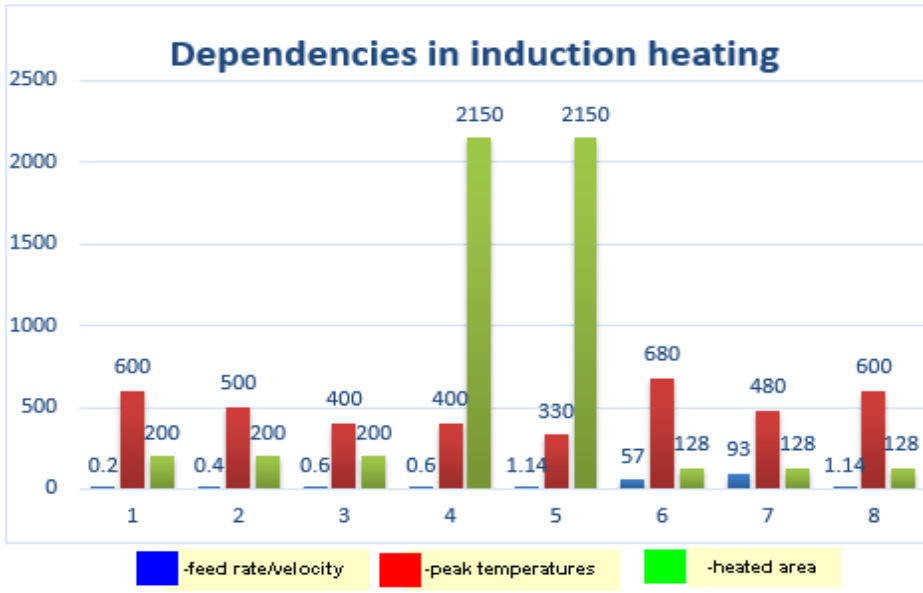


Figure 71 Dependencies in induction heating, 1-3- low frequency heating unit, 4-5 – high frequency milling coil, 6-7 high frequency turning coil in SMT, 8-HF coil for turning in pencil machine. Blue-feed rate, velocity (m/min), red- peak temperatures reached (°C), green – heated area,(mm²).

Table 2 Tabulated data for comparison of different conditions

№	Feed rate (m/min)	Temperature(°C)	Area of heating (mm ²)
1	0.2	600	200
2	0.4	500	200
3	0.6	400	200
4	0.6	400	2150
5	1.14	330	2150
№	Velocity (m/min) Turning coil	Temperature(°C)	Area of heating (mm ²)

6	57	680	128
7	93	480	128
8	1.14	600	128

From Figure 71, it is clearly seen that under smaller area required to be heated and by that, we would require much smaller heating unit, we can reach decent temperatures in much more efficient way, because flux concentration would be more narrowed, and the power transfer to the unit would be more sufficient.

Low frequency unit is out of our scope of interest as it gives very deep heat penetration which in the end results in the WP characteristics change and following deterioration of the material.

High frequency milling unit showed such results as the heated area and the coil itself were wide, at Figure 71 area was almost 10-15 times bigger than in case of other coils. Which resulted in flux dissipation into the material, so an assumption that increase in feed rate would have helped to reach desired temperatures, as under the higher feed rates upcoming material that needed to be heat would not reach higher temperatures on the deeper level, and it would not loose permeability. As a result, magnetic fluxes would have been more concentrated on the upper layers of material and the coil would not lose it efficiency. In addition, at lower feed rate heat generated on the upper layers of the WP material can dissipate into the material itself, which does not let to accumulate temperatures on the upper layers. Another proposed option is to consider further decreasing of the feed rate, there is a possibility to get to the desired level of temperatures, but heat penetration into material would be almost on the full depth, which is not considered as it eradicate desired characteristics of Mn-steels.

It can be seen from Figure 72 that after a few seconds the depth of the heat goes to 2mm, which is not suitable for the milling conditions, as a desired depth of cut should not exceed 0.5mm. To improve the MRR with implementing of the IAM, the only variables that we can configure are area of cutting and the feed rate, and for the current case one of the most logical options would be decreasing of the heated area, by that we decrease heat penetration speed, and power output is more concentrated on the area, it also gives better flux concentration. In such

case even with the smaller area, material would be soft enough for the possibility to increase the feed rate, which as result will give higher MRR.

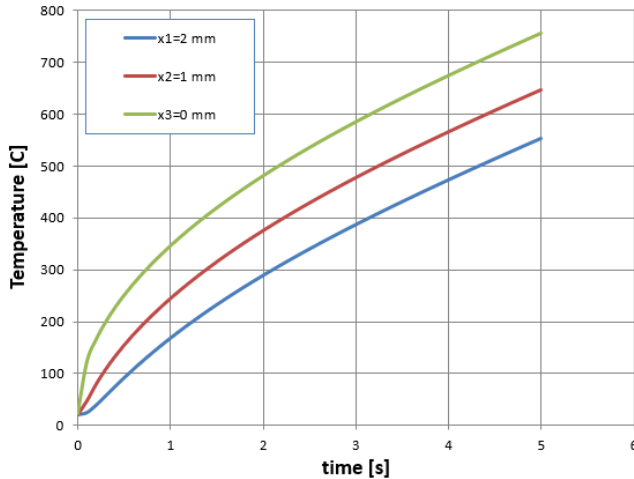


Figure 72 Simulation of heating depth dependence on time, in the current set up and the workpiece

High frequency turning unit, proved its efficiency and it was mostly related to the much-narrowed heating area, which helped to concentrate magnetic fluxes on the desired area of machining. We can see from comparing sets of 6 and 7 from Figure 71, that very high velocity is not an option also, as it requires a certain amount of time to concentrate the heat on the WP surface.

Velocity that is shown in the Table 2, for the case of 6 and 7, is calculated from the revolution made by WP and its diameter, not including the movement of the tool longitudinally, so the meaning of the velocity for the turning in case 6 and 7 is how much distance of the WP was covered at the same spot by the coil per minute, which can be interpreted as the cutting speed during the turning as it imitates movement of cutting tool across the surface of the WP. Taking in consideration that it is only calculated from the revolution motion point of view, if the feed rate is added, which means movement in the longitudinal direction of the coil unit is added, by that with the lower revolution speed, WP will reach to the higher temperatures, and in overall maintain same cutting speed. This option would be possible to

be used in case 7, as the feed rate will give the possibility of the preheating of the WP. For this case maintain revolution speed lower but by increasing the feed rate will save an overall speed of the machining, which in the end will result in better MRR. In addition, the heated width is 4mm wide, which gives possibility to use higher h_1 values resulting in bigger contact area between tool and the WP.

So as basic concept for using of the induction as preheating method for the M1 manganese steel is possible, and can be implemented to a different machining processes but it requires consideration in terms of area that need to be heated, from the initial data about area to be heated different coil design can be implemented. Because different design of the coil will produce different flux concentration pattern and time required to concentrate the fluxes would be different.

7. Conclusion

From the conducted research, following conclusions can be drawn:

1. Environment for the coils testing was built and can be further used with different types of coils and materials, with small changes in it. Different heating solutions were designed and tested on it.
2. Main factors that play role for the coil design are the area that needs to be heated and how narrowed can be the coil produced to minimize the area of the directed magnetic fluxes.
3. For the milling feed rate would play key role, because if the feed rate is too slow, spread of the heat goes too deep which in the end will result in deterioration of the Mn-steels structure, on the other hand if the speed is too fast generated heat is not enough to soften the material that needs to be machined. Methodical variation of different input parameters were suggested.
4. For the turning, cutting speed would play significant role, which is formed by rotational speed of the WP and the feed rate along the WP surface, which in the end gives us the time that coil would be on the same spot of the WP, and time for heating up the material. The time should not be too slow and should not be too fast, as it will have same aftermath as in milling. So by combining of the rotational speed and the feed rate, desired cutting speed can be reached and gain higher MRR by softening up the material and giving us more options in terms of cutting data parameters increase.
5. Universal design of the coil that can be adopted for different type of machining is hard to implement in real life set up, as a behavior in four important parameters for IAM such as area of heating, feed rate, cutting speed and penetration depth are varying for each type of the machining. For each specific production, tailored decision should be made. However, the basic concept for design was made and key factors were given.
6. On the example of high frequency coil for turning, possibility of efficient preheating of M1 manganese steel was proven.

Ability to concentrate the heat by the help of induction on the upper layers of the WP was seen, which theoretically will improve MRR for different type of processes and will even give the possibility to machine reinforced manganese steel.

In overall project proved possibility of usage of IAM for Mn-alloys and it was clearly seen on the example of HF turning coil, which gave sufficient penetration depth and the temperatures peak, so the material would deteriorate and will help to get rid of strain hardening phenomena of Mn-alloys.

8. Outlook

High frequency coil design should be adopted in a more user friendly and efficient way, more integrative approach can be done.

Further after considering such approach IAM could be implemented in different hard to cut materials processing. Size reduction of the whole set up can be done and even integrated into the lathe itself, so it can fit different WP sizes.

For the turning to increase the range of the temperatures that can be reached, and to add freedom in terms of WP size, usage of the multiple coil would be an option, so the power output on the WP would be increased and evenly spread in different part of it.

Following configuration for the turning can be manufactured and would be possible to be used. Figure 73 - Figure 75

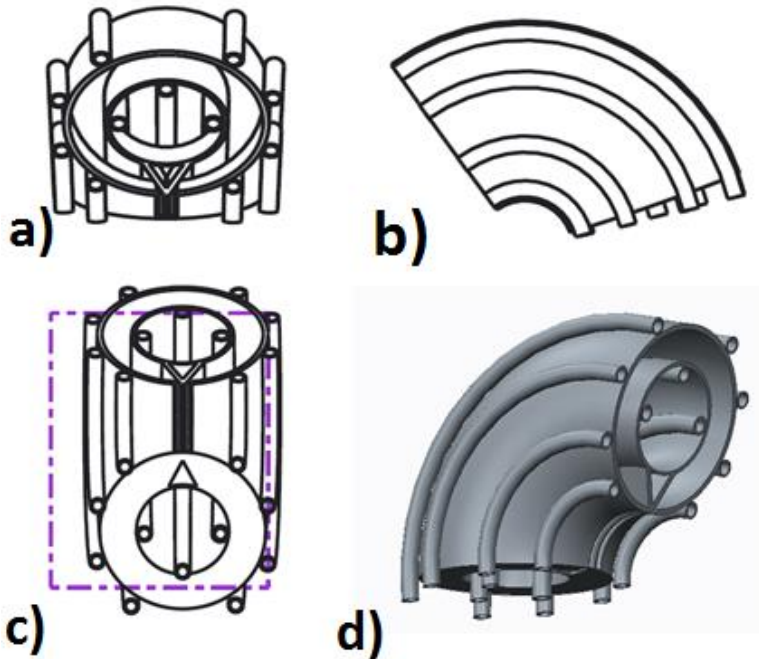


Figure 73 Suggested design for the coil. a) front view b) side view c) bottom view d) 3D model

This design will be capable of higher frequencies and the power inputs, as it can be segmented and perpendicularly mounted around the WP. As the coil will be able to concentrate the flux longer in the rotational direction of the WP, feed rate can be increased under same rotational speed, which will benefit the MRR.

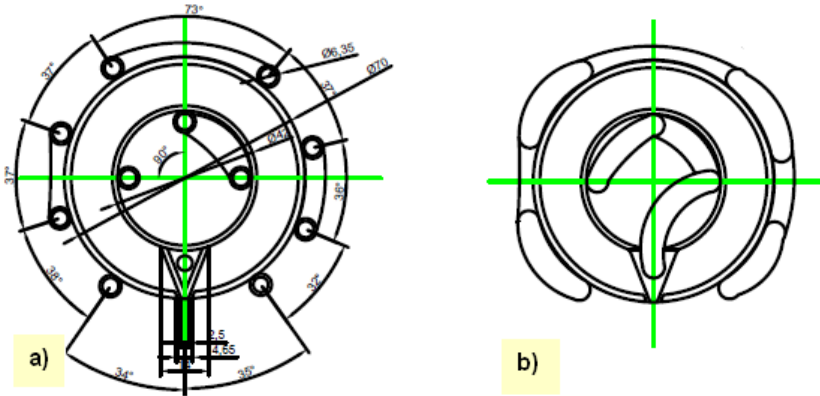


Figure 74 a) section view, b) front view

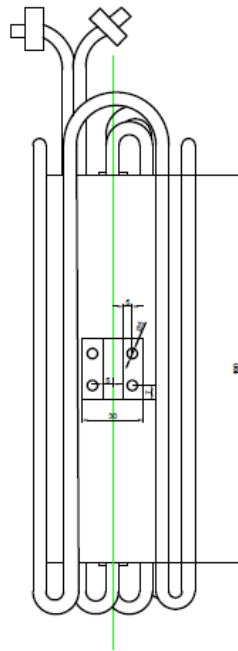


Figure 75 View from above before bending

The coil on the Figures 73-75, consist of two copper tubes with the bending angle of about 90° - 110° , small tubes in inner circle and outer circle are the tubes for cooling of the coil so the ferrite which will be molded between them would maintain suitable temperatures not to lose its permeability. 3D printed or extruded version of it also would be a good alternative for producing of it and depending on the requirements, it can either be used as the completely long body or can be later cut into segments and spread on the WP according to the production needs.

For the high frequency milling coil, redesign of the coil would be an option, to make more turns and use other type of ferrite that can withstand higher frequencies, which would be 400 kHz and above, so the flux concentration would be on the lower depth with the same speed. As under the current feed speed of the WP, we are getting severe penetration of the fluxes into WP.

Coil in different form and smaller area coverage, which would mimic the form of the milling head would be an option, with a thin width of the magnetic fluxes output.

References

- Armin Bijanzad, T. M. (2022). Heat-assisted machining of superalloys: a review. *The International Journal of Advanced Manufacturing Technology*, 118, 3531–3557.
- Baili M, W. V. (2011). Experimental Investigation of Hot Machining with Induction. *Applied Mechanics and Materials*, 62, 67–76.
- Dieringa, H. K. (2012). Magnesium Matrix Composites: State-of-the-art and whats the future. *Adv. Mat. Research* 410, 275-278.
- Eun-Jung Kim, C.-M. L. (2020). Experimental study on power consumption of laser and induction assisted machining with inconel 718. *Journal of Manufacturing Processes*(59), 411-420.
- Faulkner, L. L. (2007). *Optimal Control of Induction Heating Processes*. Columbus, Ohio: Taylor & Francis Group, LLC.
- Gupta, S. S. (2021). Fundamentals of Metal Matrix Composites. *Elsevier Inc.*
- HEMA KALIDASU, M. B. (2021). *WEAR PERFORMANCE INVESTIGATION OF METAL MATRIX COMPOSITES*. Lund: DIVISION OF PRODUCTION AND MATERIALS ENGINEERING LUND UNIVERSITY.
- J. Kopac, Z. S. (1983). The Influence of Heat Treatment on the Machinability of Highly Alloyed Manganese steels. Novi Sad: MMA.
- Jong-Tae Baek, W.-S. W.-M. (2018). A study on the machining characteristics of induction and laser-induction assisted machining of AISI 1045 steel and Inconel 718. *Journal of Manufacturing Processes*(34), 513-522.
- Kopac, J. (2001). Hardening phenomena of Mn-austenite steels in the cutting process. *Journal of Materials Processing Technology*, 109, 96±104.

- M.I. Hossain, A. N. (2008). Enhancement of machinability by workpiece preheating in end milling of Ti-6Al-4V. *JAMME* , 31(2), 320-327.
- M.S.Shramko, A. (2006). *High manganese steel , with high performance under abrasive conditions*. NPKP "PARAMI".
- Netzsch. (n.d.). <https://analyzing-testing.netzsch.com/en/products/thermal-diffusivity-and-conductivity/lfa-467-ht-hyper-flash#:~:text=The%20LFA%20467%20HT%20HyperFlash%20is%20the%20first%20flash%20lamp,series%20is%20well%20known%20for.>
- Oscar Acselrada, A. R. (2004). A first evaluation of the abrasive wear of an austenitic FeMnAlC steel. *WEAR*(257), 999-1005.
- Prof A. N. Purant, P. R. (2020). Applications of Metal Matrix Composites in Modern Engineering. *International Research Journal of Engineering and Technology (IRJET)*.
- Shirong Ge, Q. W. (2017). The impactwear-resistance enhancement mechanism of medium manganese steel and its applications in mining machines. *WEAR*(376-377), 1097-1104.
- Ståhl, J.-E. (2012). *METAL CUTTING THEORIES AND MODELS*. Lund-Fagersta: SECO TOOLS AB.
- Stjernstoff, T. (2004). Machining of some difficult to cut materials with rotary cutting tools. (p. 2.19). Stockholm: The Royal Institute of Technology, KTH.
- Turnad L. Ginta, A. N. (2009). Improved Tool Life in End Milling Ti-6Al-4V Through Workpiece Preheating. *European Journal of Scientific Research*, 27(3), 384-391.